energies

MDPI

Article

CO_2, Water and N_2 Injection for Enhanced Oil Recovery with Spatial Arrangement of Fractures in Tight-Oil Reservoirs Using Huff-'n-puff

Jie Bai [1,2], Huiqing Liu [1,2,*], Jing Wang [1,2], Genbao Qian [3], Yongcan Peng [3], Yang Gao [3], Lin Yan [4] and Fulin Chen [4]

1 State Key Laboratory of Petroleum Resources and Engineering, China University of Petroleum-Beijing, Beijing 102249, China; jaybye@163.com (J.B.); wangjing8510@163.com (J.W.)
2 MOE Key Laboratory of Petroleum Engineering in China University of Petroleum, Beijing 102249, China
3 PetroChina Xinjiang Oilfield, Karamay 834000, China; qgenbao@petrochina.com.cn (G.Q.); pyongcan@petrochina.com.cn (Y.P.); gaoyang@petrochina.com.cn (Y.G.)
4 PetroChina Research Institute of Petroleum Exploration & Development, Beijing 100083, China; linyan@petrochina.com.cn (L.Y.); Chenfulin@petrochina.com.cn (F.C.)
* Correspondence: liuhq@cup.edu.cn

Received: 2 February 2019; Accepted: 24 February 2019; Published: 1 March 2019

Abstract: Tight oil has been effectively developed thanks to artificial fracture technology. The basic mechanism of effective production through fractures lies in the contact between the fractures (both natural and artificial) and the matrix. In this paper, the natural tight cores from J field in China are used to conduct experimental studies on the different fluid huff-'n-puff process. A new core-scale fracture lab-simulation method is proposed. Woven metallic wires were attached to the outer surface of the core to create a space between the core holder and core as a high permeable zone, an equivalent fracture. Three different injecting fluids are used, including CO_2, N_2 and water. The equivalent core scale reservoir numerical models in depletion and huff-n-puff mode are then restored by numerical simulation with the Computer Modeling Group—Compositional & Unconventional Reservoir Simulator (CMG GEM). Simulation cases with eight different fracture patterns are used in the study to understand how fracture mechanistically impact Enhanced Oil Recovery (EOR) in huff n puff mode for the different injected fluids. The results showed: Firstly, regardless of the arrangement of fractures, CO_2 has mostly obvious advantages over water and N_2 in tight reservoir development in huff-'n-puff mode. Through EOR mechanism analysis, CO_2 is the only fluid that is miscible with oil (even 90% mole fraction CO_2 is dissolved in the oil phase), which results in the lowest oil phase viscosity. The CO_2 diffusion mechanism is also pronounced in the huff-'n-puff process. Water may impact on the oil recovery through gravity and the capillary force imbibition effect. N_2, cannot recover more crude oil only by elasticity and swelling effects. Secondly, the fracture arrangement in space has the most impact on CO_2 huff-'n-puff, followed by water and finally N_2. The fractures primarily supply more efficient and convenient channels and contact relationships. The spatial arrangement of fractures mainly impacts the performance of CO_2 through viscosity reduction in the contact between CO_2 and crude oil. Similarly, the contact between water in fractures and crude oil in the matrix is also the key to imbibition. In the process of N_2 huff-'n-puff, the elasticity energy is dominant and fracture arrangement in space hardly to improve oil recovery. In addition, when considering anisotropy, water huff-'n-puff is more sensitive to it, while N_2 and CO_2 are not. Finally, comparing the relationship between fracture contact area and oil recovery, oil production is insensitive to contact area between fracture and matrix for water and N_2 cases.

Keywords: tight reservoir; huff-'n-puff; fracture simulation; enhanced oil recovery; CO_2 diffusion

1. Introduction

The key dominant feature difference between a tight reservoir and a traditional reservoir lies in the tight pore. The pore throat of the porous medium of the tight reservoir is very narrow, and its movable fluid saturation is very low. The fluid flow requires a higher-pressure gradient through the pore throat (when <50 nm), and the mobility of fluids is poor [1–6], so in the development of tight reservoirs, fracturing is a key technology with an indelible contribution to oil production. The main objective of fracturing is to reconstruct the reservoir seepage formation and to achieve the purpose of the effective expansion and development of the fracture through the mechanical mechanism and provide a more efficient and convenient flow channel for the crude oil [2,7]. However, according to the evaluation of the oil production of tight reservoirs both in China and America, the production rate of tight reservoirs decreases rapidly, without a long and stable production period [2,6,8–11]. Thus, it is difficult to obtain satisfactory oil recovery only relying on the depressurization process even with fracturing.

The tight porous reservoir structure is dense, the pore throat is narrow, and at the nanometer scale, and the fluid flow is also affected by the boundary layer effect. This results in higher-pressure gradients in the flooding process in the matrix that restricts traditional flooding application in tight reservoirs [12–14], while with the existence of fractures, the breakthrough of gas/water usually occurs during the tight reservoir flooding process, so the huff-'n-puff method is considered a promising energy increasing method in tight reservoirs over the depressurization mode.

Many scholars have developed studies on effective displacement of different fluids in tight reservoirs, mainly including gas injection and chemical injection in Bakken tight oil formations [15,16]. Due to the narrow pore throat in tight reservoirs, gas injection, with its lower viscosity and larger injectivity, is considered to be much easier than water injection. CO_2 is one of the most effective injection gases for enhanced oil recovery, and the use of CO_2 to improve the recovery also serves a role of greenhouse gas storage, so it is attracting increasing attention. In the study of the enhanced oil recovery (EOR) by fluid injection, most of the studies focus on the comparison of the miscible process and immiscible process mechanisms [13,14,17–22].

In the CO_2 huff-'n-puff process, CO_2 is first injected into a producer well, then the well is shut off for soaking, finally, the well is reopened for fluids to be produced [23]. Its application to unconventional reservoirs has been investigated by lots of researchers recently [18,24–27]. The traditional EOR mechanisms of CO_2 are: (1) viscosity reduction, (2) oil swelling, (3) solution gas drive, (4) hydrocarbon extraction by CO_2. The most important operating parameters in CO_2 huff-'n-puff include injection rate and time, number of cycles, soaking time, and pressure.

Hawthorne et al. [28] explained CO_2 EOR process in tight reservoirs relatively clearly: (1) CO_2 is preferentially injected into the fractures, (2) CO_2 contacts the matrix rock through fractures, (3) CO_2 will further seep into the matrix, dominated by pressure gradients. When CO_2 dissolves in crude oil, the oil swells and its viscosity decreases, (4) oil drains into the fractures under the effect of CO_2, and (5) when the pressure gradient drops, oil transport is dominated by the concentration gradient across the matrix and the fractures.

A considerable number of scholars have also focused on the study of CO_2 in porous media and crude oil mass transfer mechanisms [15,29]. The mechanisms of CO_2 EOR in tight oil reservoirs is considered to be significantly different from those in conventional reservoirs, due to the special petrophysical properties, reservoir fluid thermodynamics, and mass transport mechanisms. Diffusion is considered to be an especially important mechanism affecting gas transportat under tight reservoir conditions, and its effect on enhanced oil recovery of tight oil cannot be neglected based on the core scale experiments.

In addition, experimental results from both 2D core slice and 3D homogeneous core scale models show that diffusion plays a significant role [30]. However, their field scale huff-'n-puff simulation model showed that convection is considered the dominating mechanism instead of diffusion. Vega carried out CO_2 injection experiments in miscible conditions [31]. The results showed that both diffusive and convective transfer mechanisms were significant.

In addition to CO_2, N_2 was also used to explore the EOR potential in tight reservoirs [32]. Cores from Eagle Ford were used in this research. Similar experiments can also be found in Li and Sheng's research [33]. The results indicated that oil recovery was improved when the soaking pressure increased. Extending soaking time can also significantly improve oil recovery. In addition, increasing huff-'n-puff cycles improved oil recovery. After six cycles, the recovery reached 30.99%.

Different from traditional steam huff-'n-and puff, cold water injection relies on the mechanism of imbibition for oil displacement in water-wet reservoirs in the presence of fractures [34,35]. This requires the rock to be water-wet. To alter the rock wettability, surfactants can be used [36–38].

In the extensive study of tight reservoirs, it is also found that the fracture formation process in tight reservoirs is complex and diverse. The fracture form (such as the Figure 1) is mainly influenced by the natural fractures and properties of the reservoir (the parameters of brittleness, modulus of elasticity, etc.) and the distribution characteristics of natural fractures [2,3,7,10,39,40]. The expansion and connection of the fractures occurs both in the plane and three-dimensional direction. The diversity in the fracture expansion and connection leads to the fact that the contact between fractures and matrix is a multi-contact relationship [39]. This undoubtedly increases the difficulty of evaluating the development effect of tight reservoirs, because the fractures are often simplified to simple uniform and single contact surfaces. In the fluid injection process, especially in huff-'n-puff mode, the mass exchange between crude oil and injected fluid is unavoidably partially ignored due to the lack of multi-contact relationships between fractures and the matrix. Research on the effect of processing under complex fracture conditions has also progressed. In Molero's research, different types of complex fractures were simulated and the effects of CO_2 huff-'n-puff evaluated. The results confirmed that the appropriate modeling of fracture geometry plays a critical role in the estimation of the incremental oil recovery. In Meng's research about imbibition effects, for fractured reservoirs the area of the water-covered-face between the fractures and matrix also had a significant effect on the oil production process. Therefore, the simulation of fractures is essential when evaluating the oil recovery in both depletion and huff-'n-puff processes [38].

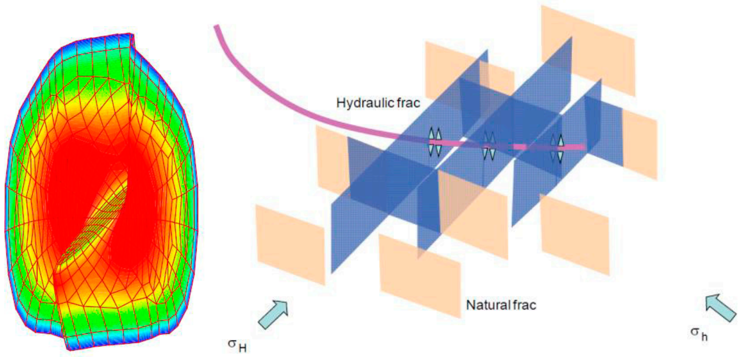

Figure 1. Nonplanar fracture model in a naturally fractured formation.

In terms of core scale experiments, cutting cores and then re-splicing them is the most common method for fracturing simulation. By cutting a complete vertical core with a saw or cutter, the core is separated in half. The fracture is then simulated by splicing the two core parts. The disadvantages of this method are usually a large fracture width (2 mm) and a loss of core and single shape of fractures. The cores also cannot be reused. Tovar et al. [30] simulated fractures by surrounding tight cores with glass beads. To prevent the loss of the glass beads, two sandstone plugs were mounted at both ends as filters. This method doesn't break the cores and keep them reusable. However, the shape of the fracture is still too single, and the whole surrounding space of the core is treated as fracture, so the rationality is questionable. In addition, the spatial arrangement of fractures still cannot be easily simulated in these methods.

On the basis of the established importance of complex fractures for tight oil huff-'n-puff processes, this research aims to mechanistically understand how complex fractures impact EOR in huff-'n-puff for different injected fluids. First, indoor core experiments were carried out, and a new fracture simulation method using woven metallic wires was proposed. Then a numerical simulation method was used to perform historical fitting of the experimental results with GMG GEM, which fully considers unconventional fluid flow, composition interaction and the mass transfer mechanism mentioned in fractured tight reservoirs. Three different injecting fluids are used, including CO_2, N_2 and water. Finally, core scale simulation cases with eight different fracture patterns are used in the study to understand how fractures mechanistically impact EOR in huff-'n-puff for different injecting fluids with a numerical method. Through this research, a more regular understanding of the influence of fracture and matrix distribution relationship on EOR process can be clear. It is of great significance for guiding fracturing construction. When selecting the optimal injected fluids corresponding to spatial arrangement fracture, theoretical support can also be obtained from this study.

2. Methodology

2.1. Experiments

The core plug used in this experiment was from the J Oilfield with a water-wet wettability. Three cores were selected to perform the huff-'n-puff process with CO_2, water and N_2. For the experimental system, a degassed crude oil is selected, so the weighing method is adopted to measure the amount of oil produced. Then the oil recovery of each round is calculated. The length is 5 cm with a diameter of 2.5 cm. The permeability is about 0.0375 mD, and porosity is 17.5%. Three cores are selected and their properties are listed in Table 1.

Table 1. Experimental core data.

Core Number	Porosity, %	Gas Permeability, mD	Liquid Permeability, mD
1	0.177513	0.0356	0.02835
2	0.175812	0.03691	0.0304
3	0.173267	0.03994	0.0339
Average	0.175531	0.037483	0.030883

In this paper, a new method for the simulation of core-scale fractures was designed. As shown in Figure 2, woven metallic wires attached to the outer surface of the core create a space between the core holder and core as a high permeable zone, equivalent to a fracture. The shape of the metallic cloths can be adjusted to mimic different fracture geometries and relative positions in space. In order to ensure the same fracture area, the same metal meshes were used and the cropped different shaped metal meshes kept at the same weight. The flow chart is shown in Figure 3.

In a specific experimental process, first, we wash, dry and weigh the tight core. The core is saturated with a vacuum saturate. The weight of the core before and after oil saturation is measured separately to determine the weight of oil. Finally, 3.5 mL oil is saturated in the tight core. Then, the core is placed into the core holder. A confining pressure of 30 MPa was applied to the core holder by the hand pump. Then it was saturated with an extra 1.2 mL of oil when initial pressure reached 30 MPa. The viscosity of the oil is 6 mPa·s at 60 °C. The entire system was placed in an incubator at 60 °C. Thus, the core scale tight reservoir system has been simulated using a lab method.

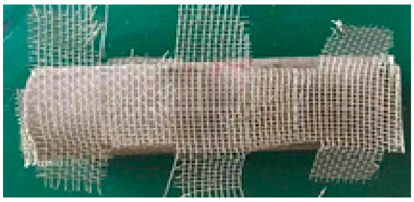

(**a**) fracture arrangement in case 2 (ij profile)

(**b**) fracture arrangement in case 2 (ik profile)

(**c**) fracture arrangement in case 4 (ij profile)

(**d**) fracture arrangement in case 4 (ik profile)

Figure 2. Basic fracture-matrix core.

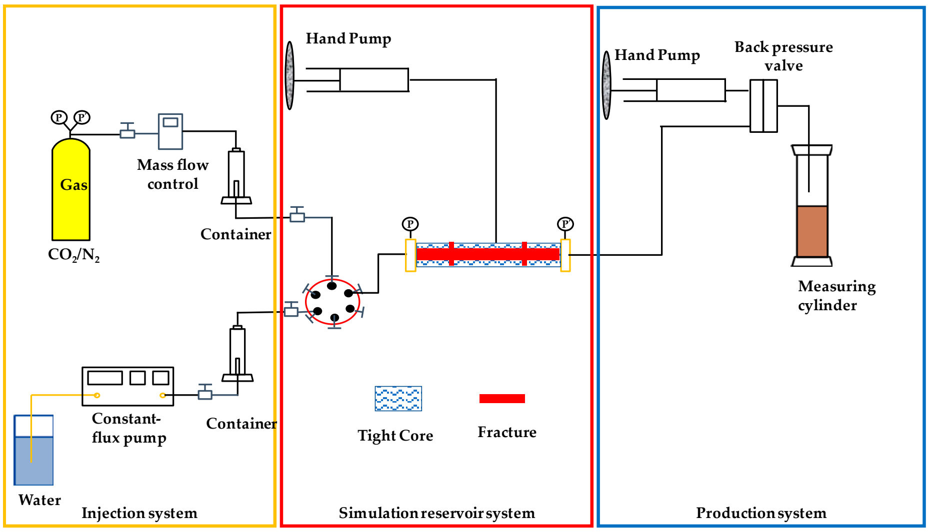

Figure 3. Flowchart of the huff-'n-puff experiments.

The injection scheme for the huff-'n-puff process is as follows: first, reduce the core pressure from an initial pressure of 30 MPa to 5 MPa. Then, inject CO_2/N_2/Water until the BHP reaches 40 MPa. The huff-'n-puff is repeated 12 times. The oil produced in the depletion process and CO_2/N_2 huff-'n-puff processes can be directly weighed, while in water huff-'n-puff, the water should be dried before weighing the produced oil.

The lab method can only provide practical oil recovery data. Subjected to laboratory conditions, the internal pressure and saturation, as well as other properties of fluids, are difficult to measure during a core-scale huff-'n-puff process. Then based on the experimental results, the parameters of relative permeability and fracture permeability are determined by fitting historical experimental data (shown in Figure 4). Finally, the numerical simulation method is used for more detailed analysis and research in the tight core production process.

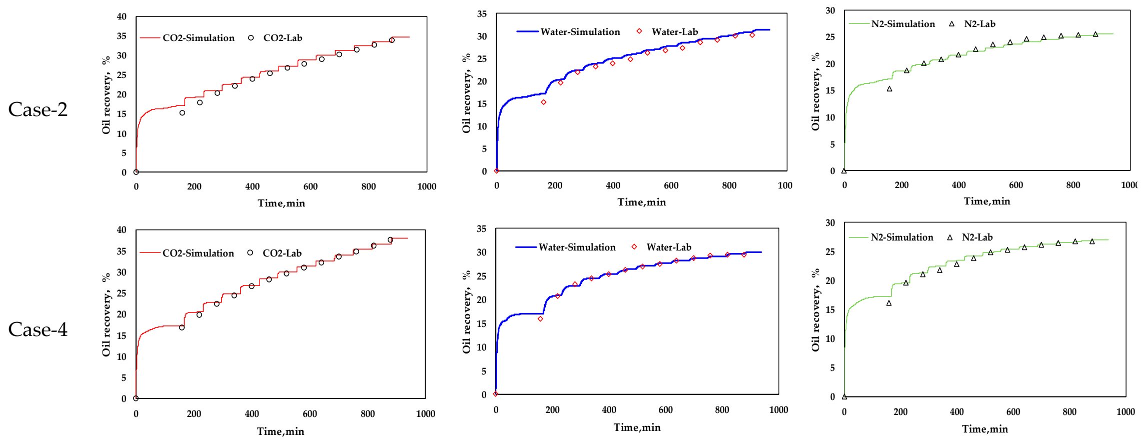

(**a**) CO_2 (**b**) N_2 (**c**) Water

Figure 4. Comparisons of oil recovery between lab data and huff-'n-puff simulation.

2.2. Numerical Simulation

2.2.1. Reservoir Simulation Model

To investigate the several mechanism effect on oil recovery, a Cartesian grid model is built in CMG GEM [41] based on the core experiments. The governing equation describing the mass balance of component *i* in the oil/gas phases is given by the following expression [15], including the cumulative term of component *i* in the rock and fluid phases, and the convection, dispersion and molecular diffusion term of component *i* in phase *j*:

$$\frac{\partial}{\partial t}[(1-\phi)\rho_s w_{is} + \phi \sum_{j=1}^{n} \rho_j S_j w_{ij}] + \vec{\nabla}\cdot[\sum_{j=1}^{N_p} \rho_j w_{ij} u_j - \phi \rho_j S_j K_{ij} \nabla w_{ij}] - r_i = 0, \quad i = 1,2,\ldots N_c, \quad j = 1,2,\ldots N_p, \tag{1}$$

where ϕ is the porosity of the tight matrix, ρ_s is the density of the tight matrix, ρ_j is the density the of *j* phase, S_j is the saturation of phase *j*, w_{is} is the fraction of component *i* that precipitates in the tight matrix rock, w_{ij} is the fraction of component *i* in the phase *j*. r_i is the injection or production rate as a source or sink term, N_p is the total number of phases, N_c is the total number of components, u_j is the flow velocity, which is defined based on Darcy's law as:

$$u_j = \frac{Kk_{rj}}{\mu_j}(\nabla p_j - \rho_j g) \tag{2}$$

In particular when both oil and water phases exist, the capillary pressure also has effect on the flow velocity, and the equation is described as:

$$u_w = \frac{Kk_{rw}}{\mu_w}(\nabla p_w + \nabla p_{\mathrm{cow}}(S_{\mathrm{w}}) - \rho_w g) \tag{3}$$

where K is the formation permeability, k_{rj} is the relative permeability of phase *j*, p_j is the pressure of phase *j*, and μ_j is the viscosity of phase *j*. K_{ij} is the dispersivity coefficient of component *i* in the phase *j*,which is defined as:

$$K_{ij} = \frac{D_{ij}}{\tau} + \frac{\alpha_l |u_l|}{\phi S_l} \tag{4}$$

where τ is the tortuosity of the tight matrix, D_{ij} is the diffusion coefficient of component *i* in phase *j*, and α_l is the dispersity coefficient of fluid *j* in different directions.

D_{ij} (its units are cm^2/s) can be calculated based on the Sigmund correlation [42]. The diffusion in water phase is ignored. The diffusion coefficient D_{ik} is calculated by:

$$D_{ik} = \frac{\rho_j^0 D_{ik}^0}{\rho_j}(0.99589 + 0.096016\rho_{jr} - 0.22035\rho_{jr}^2 + 0.032674\rho_{jr}^3) \tag{5}$$

where $\rho_j^0 D_{ik}^0$ is the zero-pressure limit of the product of density and diffusivity, which can be calculated by:

$$\rho_j^0 D_{ik}^0 = \frac{0.001853T^{0.5}}{\sigma_{ik}^0 \Omega_{ik} R}\left(\frac{1}{M_i} + \frac{1}{M_k}\right)^{0.5} \tag{6}$$

where T is the absolute temperature (K), σ_{ik} is the collision diameter (Å), Ω_{ik} is the collision integral of the Lennard-Jones Potential, R is the universal gas constant, and M_i is the molecular weight of component i. These parameters can be calculated by the following equations [43]:

$$\sigma_i = (2.3551 - 0.087\omega_i) \times \left(\frac{T_{ci}}{P_{ci}}\right)^{1/3} \tag{7}$$

$$\varepsilon_i = \kappa_B(0.7915 - 0.1963\omega_i)T_{ci} \tag{8}$$

$$\sigma_{ij} = \frac{\sigma_i + \sigma_j}{2} \tag{9}$$

$$\varepsilon_{ij} = \sqrt{\varepsilon_i \varepsilon_j} \tag{10}$$

$$T_{ij}^* = \frac{\kappa_B T}{\varepsilon_{ij}} \tag{11}$$

$$\Omega_{ij} = \frac{1.06036}{(T_{ij}^*)^{-0.15610}} + \frac{0.19300}{\exp(-0.47635T_{ij}^*)} + \frac{1.03587}{\exp(-1.52996T_{ij}^*)} + \frac{1.76464}{\exp(-3.89411T_{ij}^*)} \tag{12}$$

where ω is the acentric factor, P_c is the critical pressure (atm), T_c is the critical temperature (K), ε is the characteristic Lennard-Jones energy and κ_B is the Boltzmann constant:

$$\kappa_B = 1.3805 \times 10^{-16} ergs/K \tag{13}$$

ρ_{jr} is the reduced density, which can be calculated by:

$$\rho_{jr} = \rho_j\left(\frac{\sum_i^{N_c} y_{ij} V_{ci}^{5/3}}{\sum_i^{N_c} y_{ij} V_{ci}^{2/3}}\right) \tag{14}$$

V_{ci} is the critical volume of component i, y_{ij} is the mole fraction of component i in phase j. Nc is the total number of components. The diffusion coefficient of component i in the mixture D_{ij} is defined as:

$$D_{ij} = \frac{1 - y_{ij}}{\sum_{i \neq k} \frac{y_{ij}}{D_{ik}}} \tag{15}$$

In this paper, the core scale reservoir depletion and huff-'n-puff process were simulated with CMG GEM based on the partial differential equation (PDE) of Equation (1).

2.2.2. Reservoir Model Description

The matrix is rectangular with dimensions of 5 × 2.5 × 2.5 cm (Figure 5). This core is divided into 10 × 5 × 5 gridblocks with dimensions of 0.5 cm × 0.5 cm × 0.5 cm. The matrix is assumed to be homogeneous and isotropic with a porosity of 0.175 and permeability of 0.03 mD. The relative permeability curve inside the matrix is given in Figure 6. Two layers of grid in each direction with dimensions of 0.1 cm × 0.5 cm × 0.5 cm, 0.5 cm × 0.1 cm × 0.5 cm and 0.5 cm × 0.5 cm × 0.1 cm are added to the periphery of the matrix model to serve as the grid space of the fracture, and thus the total number of model grids is 12 × 7 × 7.

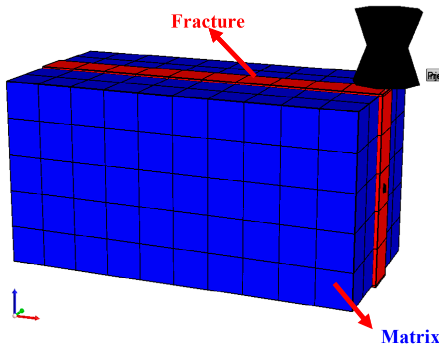

Figure 5. Basic Fracture-Matrix Model in CMG.

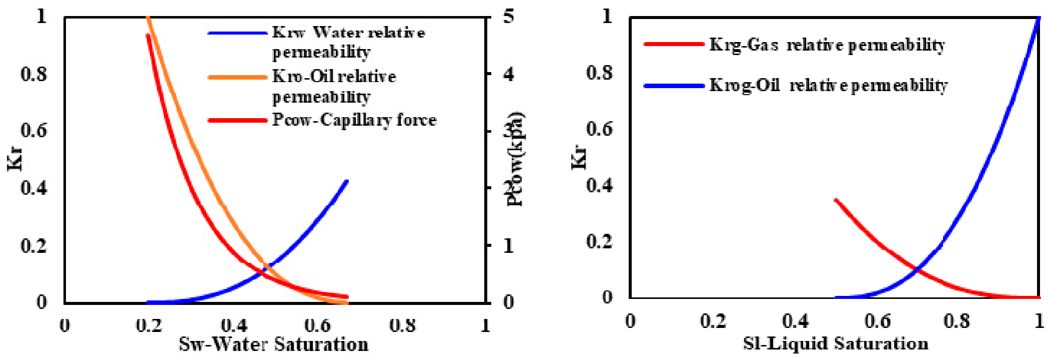

(**a**) Water/oil relative permeability (**b**) Liquid/gas relative permeability

Figure 6. Relative permeability curve of the matrix.

The fractures are assumed to be thin highly permeable passages covering the surface of the core sample matrix. These assumptions are experimentally possible as shown in Figure 5. Woven metallic wires attached to the outer surface of the core create space between the core holder and core as a high permeability zone, an equivalent fracture. The shape of the metallic cloths can be adjusted to mimic different fracture geometries and relative positions in space.

Validating the model with experimental data is critical to ensure that the simulation results are correct. In the history matching work, the main adjustment parameters are the relative permeability curves and the fracture permeability. The porosity of the fractures is assumed to be 0.5 and permeability 50 mD through the history fitting of the experimental data. The relative permeability inside the matrix and the fractures are shown in Figures 6 and 7.

The injected fluids for huff-'n-puff in this paper are CO_2, N_2 and water. The initial oil and water saturations are 0.8/0.2. The initial pressure is 30MPa. The oil viscosity is 6 mPa·s. The CO_2 diffusion coefficient is set based on published simulated and laboratory measurements [15,30,44,45]. Other initial reservoir properties can be found in Table 2. The phase behavior of water/oil, water/oil/CO_2, and water/oil/N_2 are modeled with the Peng-Robinson equation of state. Inputs for the EOS model is given in Tables 3 and 4. The initial oil components are provided by the J field, and shown in Table 5. The well is located at (12,4,4) as indicated in Figure 5. The injection scheme for the huff-n-puff process are as follows: first, depletion and pressure to 5 MPa. Then, inject CO_2/N_2/Water until BHP reaching 40 MPa. Huff-'n-puff is repeated 12 times.

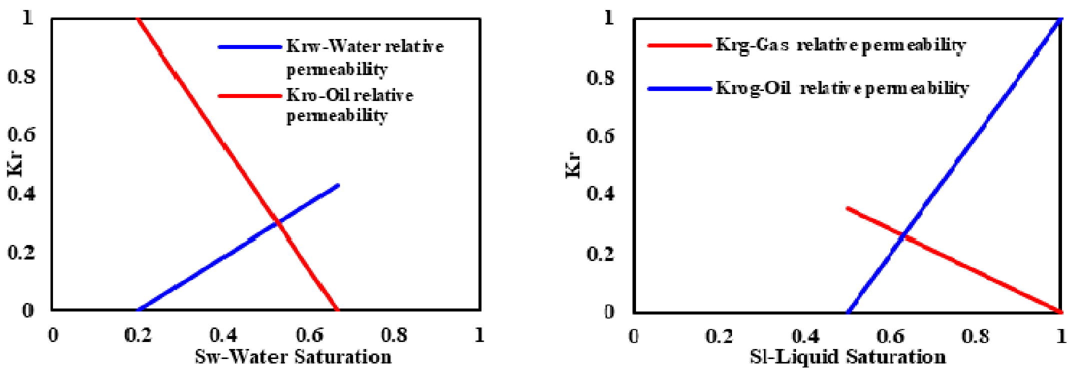

(**a**) Water/oil relative permeability (**b**) Liquid/gas relative permeability.

Figure 7. Relative permeability curve of the fracture.

Table 2. Basic reservoir properties in the numerical model.

Parameter	Value	Unit
Initial reservoir pressure	30	MPa
Porosity	0.175	-
Oil viscosity	6	mPa·s
Soak pressure	40	MPa
Soak time	45	min
Production time	6	min
Cycle number	12	-
Temperature	60	°C
Initial water saturation	0.2	-
Matrix permeability	0.03	mD
Fracture permeability	50	mD
CO_2 diffusion coefficient	0.0005	cm^2/s

Table 3. Binary interaction parameters.

Component	CO_2	C1	C4	C7	C12	C19	C30	N_2
CO_2								
C1	0.103							
C4	0.1317	0.013						
C7	0.1421	0.0358	0.0059					
C12	0.1501	0.0561	0.016	0.0025				
C19	0.1502	0.0976	0.0424	0.0172	0.0067			
C30	0.1503	0.1449	0.0779	0.0427	0.0251	0.0061		
N_2	−0.02	0.031	0	0	0	0	0	

The relative arrangement of matrix and several fractures are modeled on a core scale with CMG GEM. Table 6 lists the core-scale tight oil-reservoirs with the same contact area between fractures and cores, but with different fracture spatial arrangements.

Table 4. Component properties and composition.

Component	Pc/atm (atm)	Tc (K)	Acentric Factor	Mol. Weight (g/gmole)	Volume Shift	Crit. Volume (m^3/kgmole)	Omega A	Omega B	Specific Gravity (SG)	Tb (°C)	Parachor
CO_2	72.80	304.20	0.23	44.01	−0.09	0.10	0.46	0.08	0.60	−102.51	126.49
C1	45.24	189.67	0.01	16.21	−0.15	0.09	0.46	0.08	0.35	−161.15	40.38
C4	43.49	412.47	0.15	44.79	−0.09	0.23	0.46	0.08	0.80	−17.09	128.86
C7	37.69	556.92	0.25	83.46	−0.01	0.35	0.46	0.08	0.95	86.79	242.85
C12	31.04	667.52	0.33	120.52	0.06	0.50	0.46	0.08	1.05	176.75	345.92
C19	19.29	673.76	0.57	220.34	0.16	0.89	0.46	0.08	1.30	217.98	593.49
C30	15.38	792.40	0.94	321.52	0.21	1.06	0.46	0.08	1.50	331.76	799.68
N_2	33.50	126.20	0.04	28.01	0.00	0.09	0.00	0.00	0.81	−195.75	41.00

Table 5. Oil composition in the simulation model.

Competent	Percent/%
ZGLOBALC 'N_2'	1
ZGLOBALC 'CO_2'	0.01
ZGLOBALC 'C1'	23.79
ZGLOBALC 'C4'	4.38
ZGLOBALC 'C7'	11.26
ZGLOBALC 'C12'	36.18
ZGLOBALC 'C19'	16.51
ZGLOBALC 'C30'	7.87
Sum	100

Table 6. Settings of fracture contact relationships.

Fracture Pattern	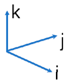	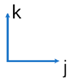 ***I* = 1**	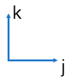 ***I* = 10**	Remarks
0	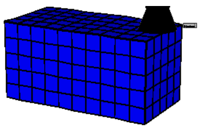	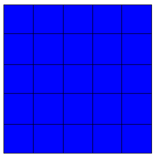	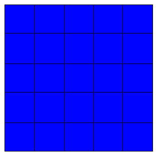	Baseline
1	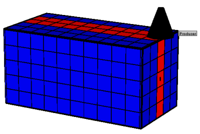	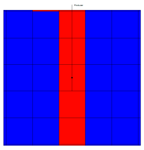	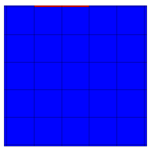	Scattered fracture-1
2	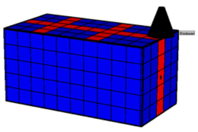	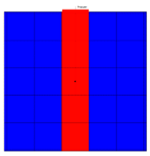	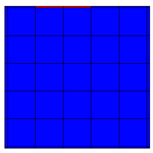	Scattered fracture-2
3	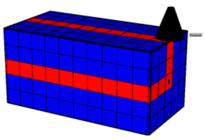	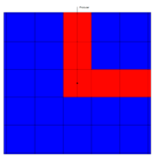	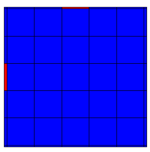	Scattered fracture-3
4	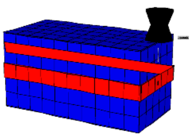	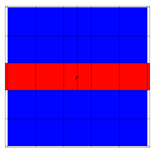	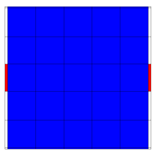	Scattered fracture-4
5	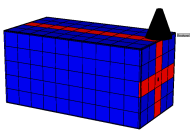	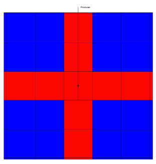	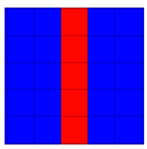	Near well

Table 6. *Cont.*

Fracture Pattern	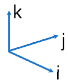	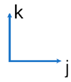 ***I* = 1**	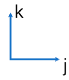 ***I* = 10**	Remarks
6	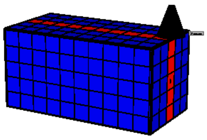	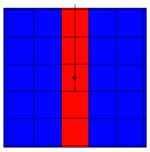	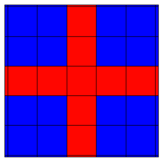	Far well
7	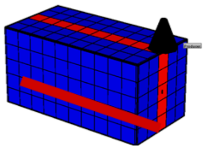	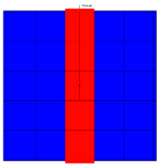	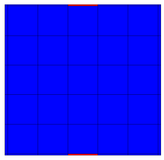	Relationship with Kv and Gravity

3. Results

3.1. Depletion and Huff-'n-puff with Different Fluids

3.1.1. Depletion Mode

By comparing the simulation results of the different fracture mode cases (Figure 8), it is found that in the depressurization period, the existence of fractures is significant for the enhanced oil process. With the same contact area between fracture and matrix, the cases with fractures have approximately 18% higher oil recovery than the case without any fracture. Figure 9 shows the pressure distribution in several cases. Without fractures, the pressure drop is not obvious. The pressure change area in the cases with fracture is wider and the pressure drop is more significant, especially in Case-4. This shows that the fractures supply the more efficient and convenient channels and contact relationships.

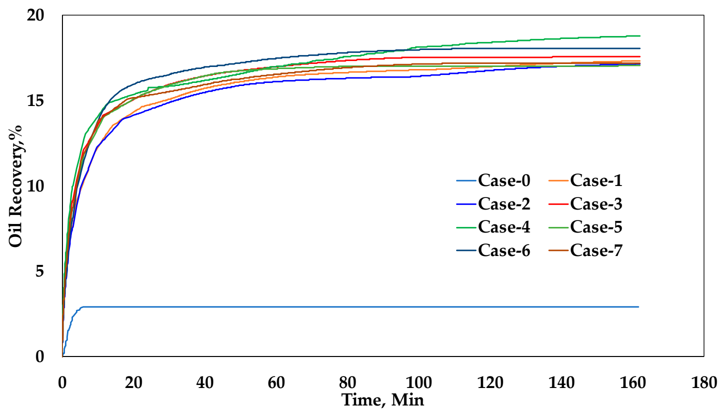

Figure 8. The comparison of oil recovery in fracture and no-fracture conditions.

In the depletion mode, crude oil flows mainly by the pressure drop caused by elastic energy, and there is no contact between other fluids and crude oil in the matrix through fractures. Therefore, in the case of depletion mode, when fractures have the same contact area with spatial arrangement, the obvious difference in oil recovery cannot be observed.

Case-4 represents the most typical contact relationship between horizontal well fracturing artificial fracture and tight matrix without natural fracture. Case-4 is consistent with the experimental scheme. Figure 9 shows that the fracture type in Case-4 has the best pressure spread effect. In the next study, Case-4 is used as the basis for comparing different fluid using huff-'n-puff.

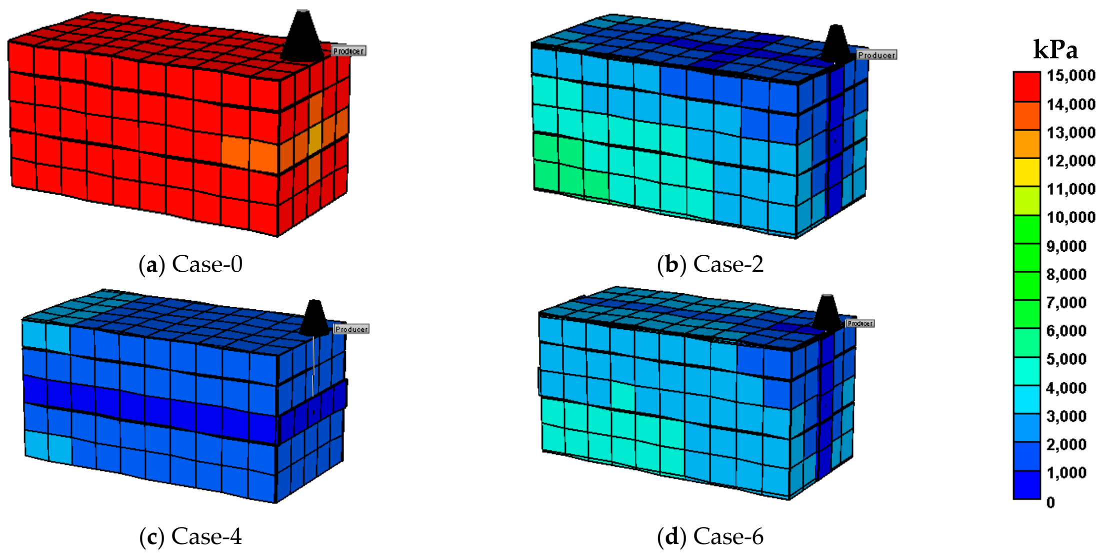

Figure 9. Pressure comparison between different scattered fractures in the depletion process.

3.1.2. Comparison of CO_2, N_2 and Water as Injecting Fluids for Huff-n-puff

- Oil recovery comparison

In this part, Case-4 is used to illustrate the mechanisms of using CO_2, N_2 and water for the huff-'n-puff process. Figure 10 shows the oil recovery factor on surface conditions by using the three different injecting fluids. CO_2 was able to enhance oil recovery by 21% after depletion, water by 13%, and N_2 by 10% so CO_2 has obvious advantages over water and N_2.

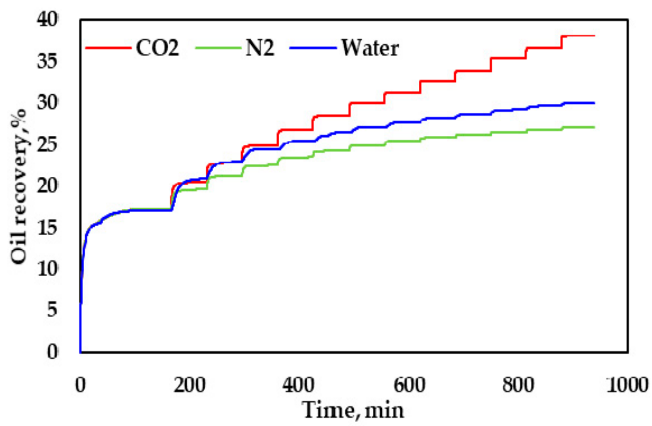

Figure 10. Oil recovery comparison of different fluids (Case-4).

- Gas/liquid injection volume

Firstly, injection fluid volume under the reservoir conditions was selected as a comparison index for the injectivity (Figure 11) to evaluate the EOR effect of different fluids.

From the comparison it can be found that the injectivity of N_2 is the highest among the three fluids, but its impact on EOR is the least. CO_2 has the secondary injectivity with the best EOR effect. The injected volume of water is the least, but with a moderate oil recovery.

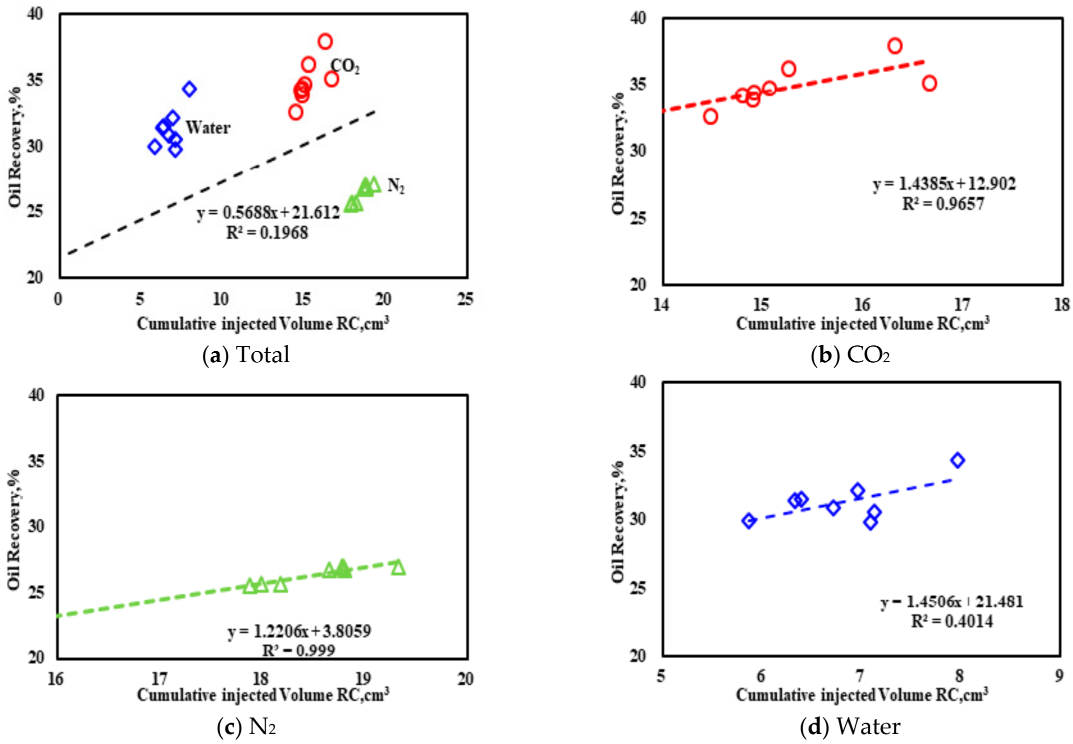

Figure 11. Relationship between injection volume RC and oil recovery in huff-'n-puff mode.

Then, we also found the relationship between the volume of the accumulative injection of fluid and the oil recovery under the reservoir conditions of different fluids (CO_2, N_2 and water) cannot be satisfactorily correlated (shown in Figure 11a). It shows that that the injectivity is only part of the basis for the EOR effect of fluids. Because of the obvious difference of EOR mechanism among the three fluids, the oil recovery only shows a good linear relationship with cumulative injected volume under reservoir conditions in same fluid cases (shown in Figure 11b–d).

The following is a detailed comparison of EOR processes of different fluids, to analyze how distributions of the fractures mechanistically affect the performance of the three different injectants:

- Viscosity profile and CO_2 concentration in oil phase

To further understand the EOR mechanisms of the three different injecting fluids, the influential factors in oil recovery are examined. One of the most important factors is the viscosity of the oil phase, which is affected by the thermodynamic conditions and oil composition. Figure 12 shows the viscosity of oil phase during the soaking process in the 12th cycle by using the three different fluids. It can be found that the effect of CO_2 on crude oil viscosity reduction is very significant, especially the viscosity of crude oil near the well and near the interface of fractures has the most significant change from the initial 6 mPa·s to about 1 mPa·s. However, N_2 is also mixed as a gas during the contact with crude oil, but there is no obvious viscosity reduction effect. After the water injection, the viscosity of crude oil may even increase to 7.5 mPa·s.

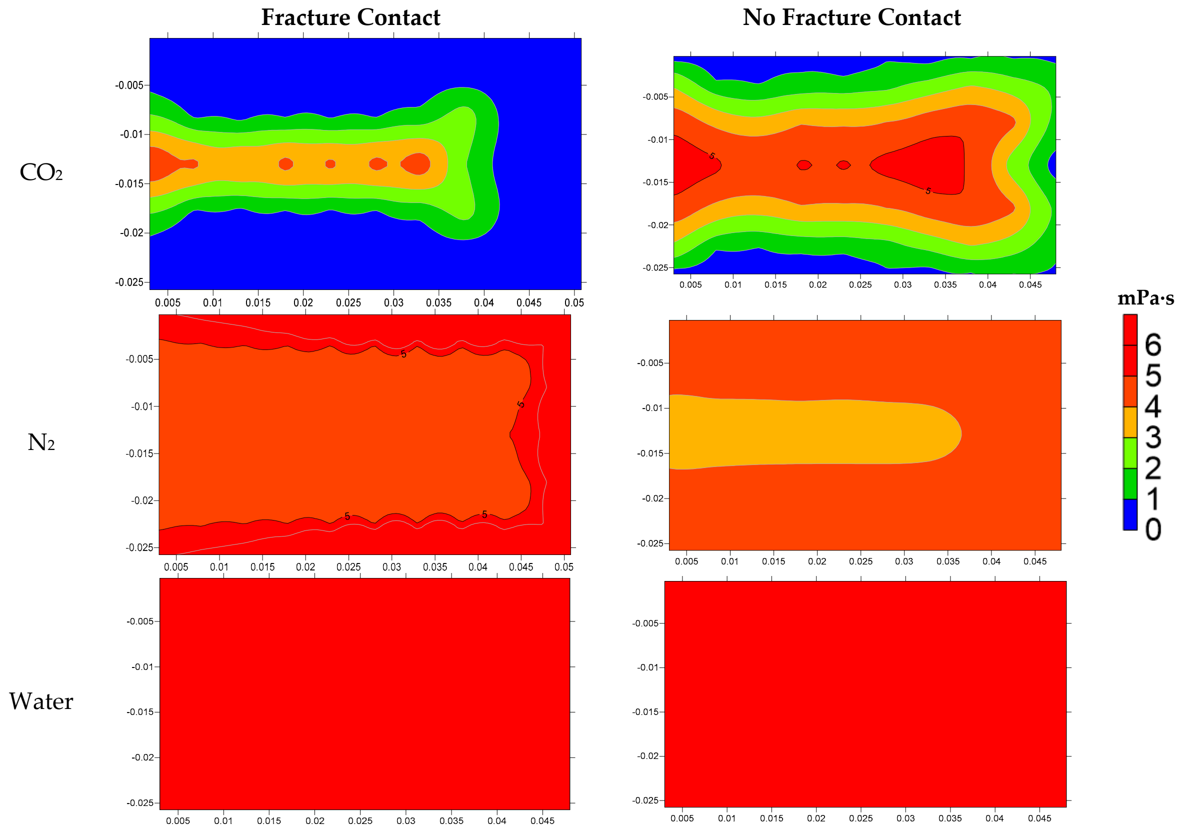

Figure 12. Oil viscosity of different fluids in Case-4 in soaking process (ij profile).

CO_2 is only fluid that is miscible with oil (even at 90% mole fraction with CO_2 in the oil phase as shown in Figures 13–15). The solubility of CO_2 results in the lowest oil phase viscosity of the three cases. In contrast, N_2 mainly exists in the gas phase and is much less soluble in the oil phase compared to CO_2. Water does not dissolve in the oil and water mainly enhances oil recovery through capillary force, gravity and elasticity displacement.

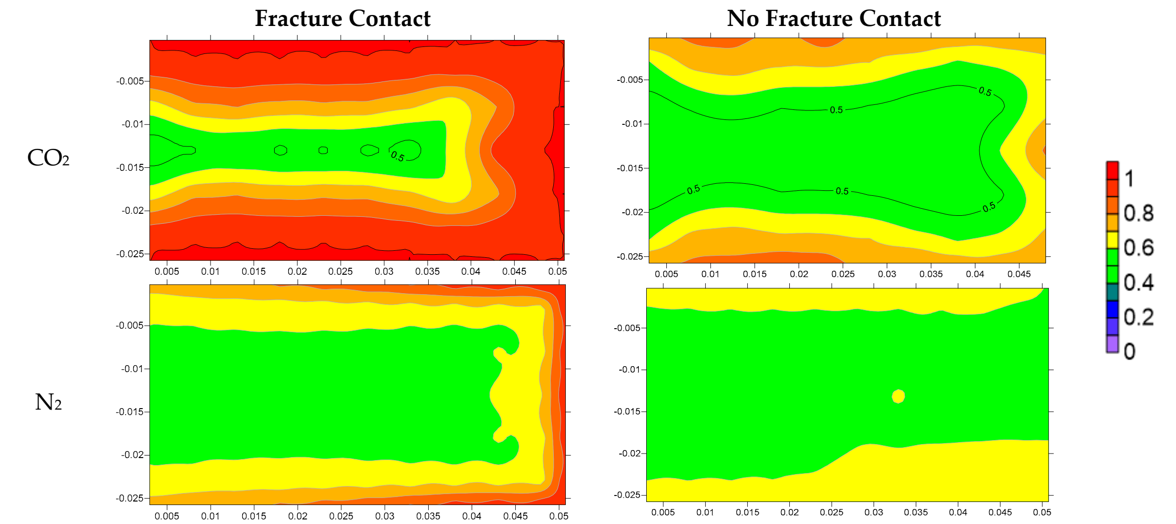

Figure 13. Mole fraction of injection fluid in oil in Case-4 in soaking process (ij profile).

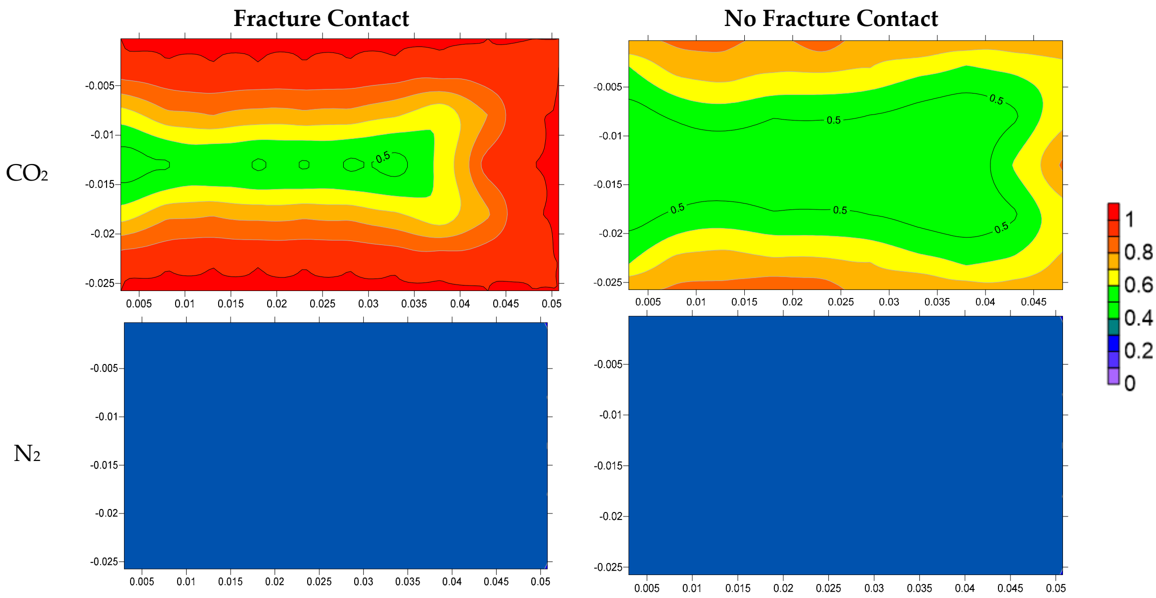

Figure 14. Mole fraction of injection fluid in oil in Case-4 in soaking process (ij profile).

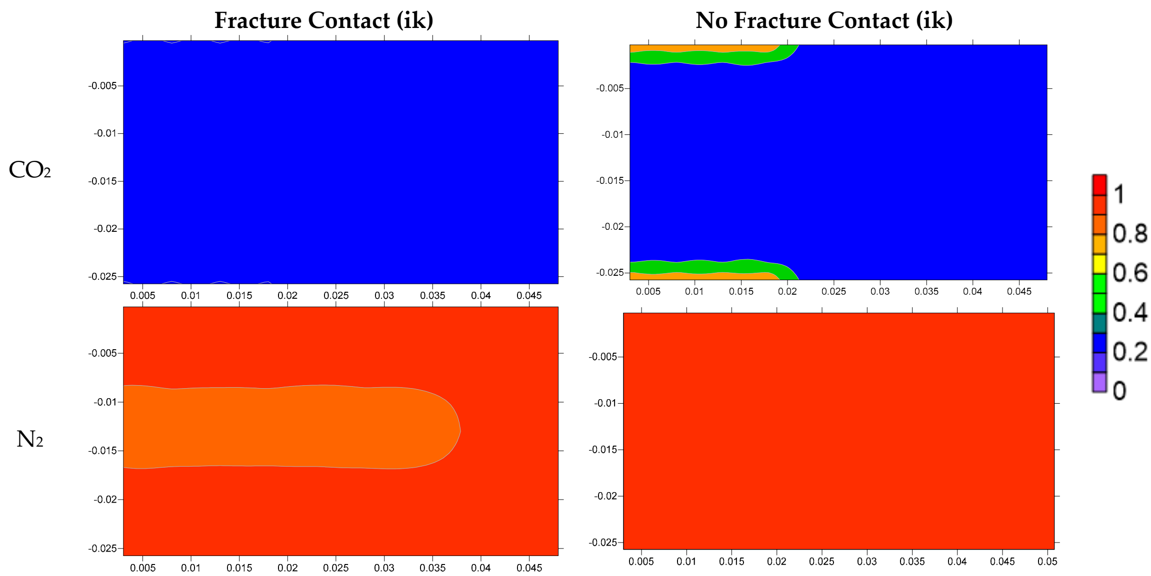

Figure 15. Mole fraction of injection fluid in gas in Case-4 in soaking process (ij profile).

Figure 16 shows the produced components of all three cases. CO_2 gives the most incremental C19 and C30 compared to depletion. However, in the water case, more C7 are produced, leaving a deprived heavy mass that causes an increase in the viscosity of the crude oil. N_2 has the least incremental effect on oil components in all carbon number ranges.

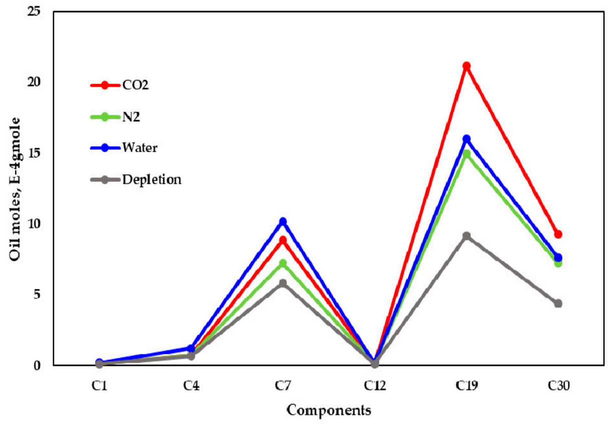

Figure 16. Production component comparison in Case-4.

- Oil swelling

The mixture of gas and crude oil will cause a volume expansion of crude oil. Figure 17 shows that the volume expansion of crude oil under reservoir conditions is most obvious after CO_2 injection, and N_2 has only a slight expansion effect on oil volume. When injecting water, the oil is compressed and its volume in reservoir condition decreased. Based on the expansion mechanism, CO_2 showed much better displacement performance than N_2 and water.

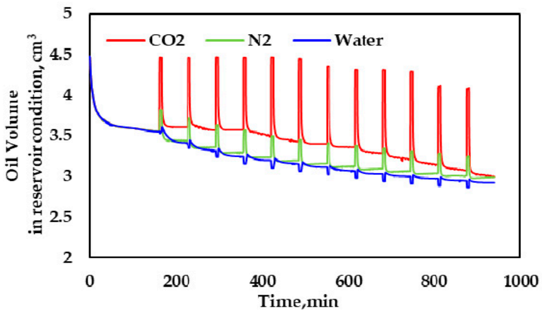

(**a**) oil volume in reservoir condition

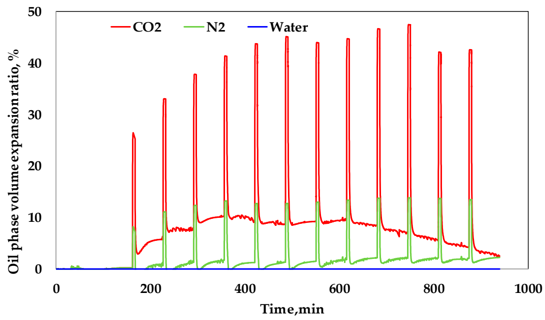

(**b**) oil volume expansion ratio in reservoir condition

Figure 17. Oil volume in reservoir conditions comparison in Case-4.

- Saturation profile and relative permeability profile

Another influential factor is the relative permeability of the oil phase. Figure 18 shows the relative permeability of the oil phase in the same production process in the 12th cycle. Figure 19 shows the oil, water and gas saturations at the same time. It can be seen with similar oil saturation, the relative oil relative permeability in the CO_2 and water case is much higher than the N_2 case. This is a consequence of the much lower relative permeability to liquid with the existence of gas phase. Based on the gas/liquid relative permeability curve, when two-phase flow occurs, the gas flows more easily than the liquid. Because the gas-liquid two-phase flow area is obviously narrower than the oil-water two-phase flow area (Figures 6 and 7).

From the saturation distribution of production stage in Figure 19, it can be seen that for gas huff-'n-puff, oil saturation in some areas is even higher than that in water huff-'n-puff. In water huff-'n-puff, because of the wider two-phase flow area of water and oil, the overall saturation decline area is larger. However, influenced by comprehensive mechanisms, water's EOR effect is still not as good as CO_2 with viscosity reduction mechanism, but better than N_2.

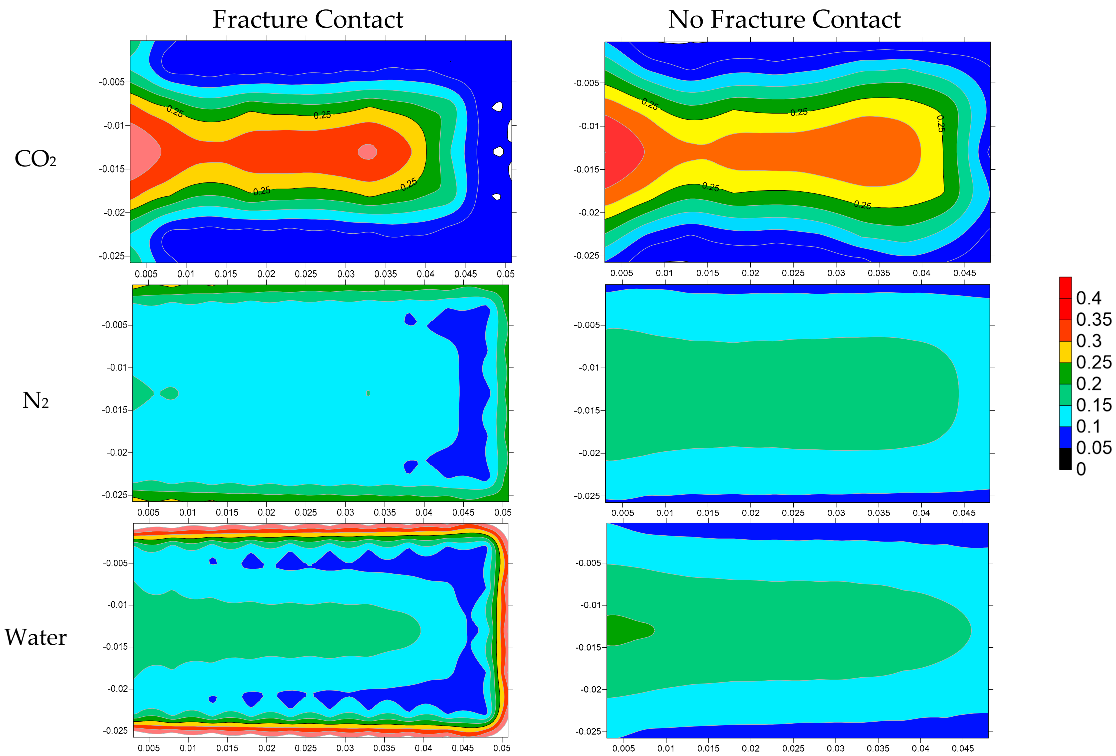

Figure 18. Oil relative permeability of different fluids in Case-4 in the production process (ij profile).

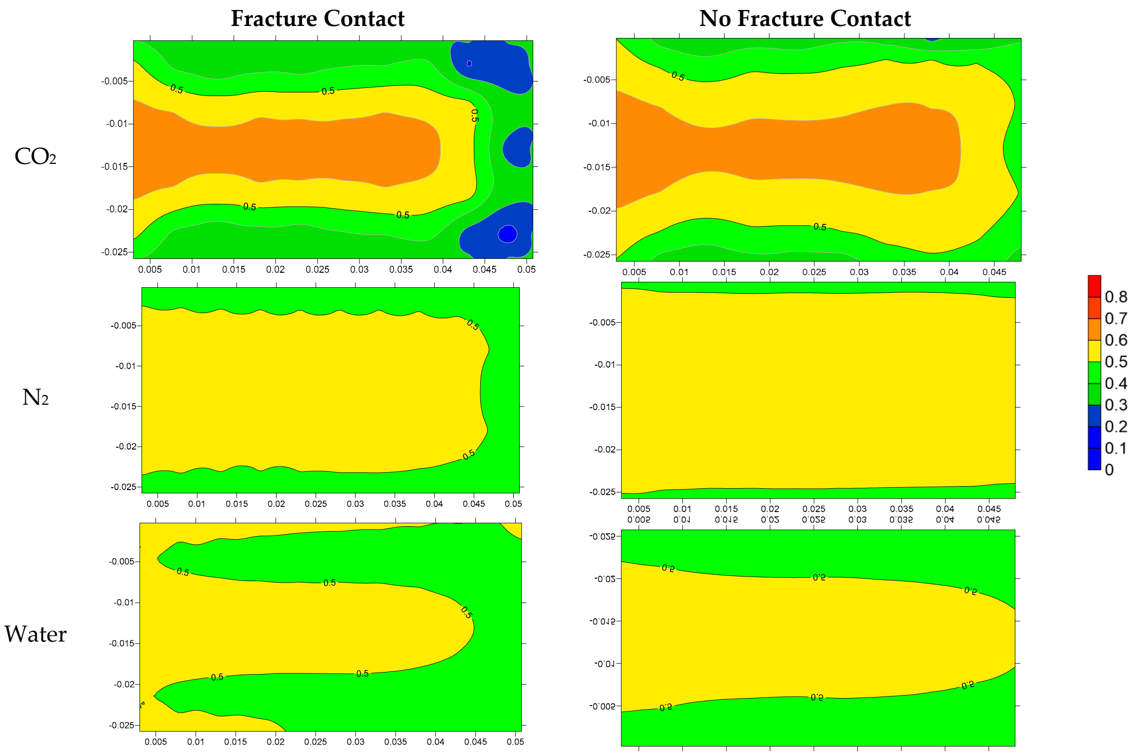

Figure 19. Oil saturation of different fluids in Case-4 in production process (ij profile).

- CO_2 diffusion

Figure 20 shows that the oil recovery considering the CO_2 diffusion effect at 0.005 cm^2/s is 1.42% higher than the cases without considering it. Figure 21 compares the CO_2 global mole fraction distribution profile with and without CO_2 diffusion. From the profile, the matrix grids have higher

CO_2 mole fraction with consideration of CO_2 diffusion, which indicates that more CO_2 may enter into the tight matrix from fractures to mix with the crude oil. Therefore, in order to accurately enhance the oil recovery effect of CO_2 in the tight reservoir simulation model, CO_2 diffusion effects cannot be ignored. On the basis of CO_2 diffusion to improve CO_2 EOR, a reasonable value of diffusion coefficient is critical for the reasonable evaluation of oil recovery in CO_2 huff-'n-puff.

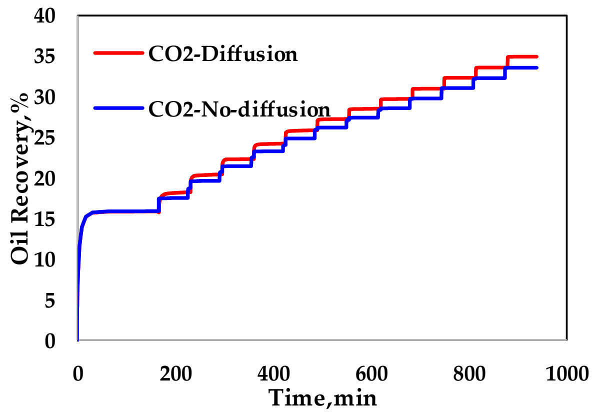

Figure 20. Oil recovery comparison of CO_2 huff-'n-puff with and without diffusion (Case-4).

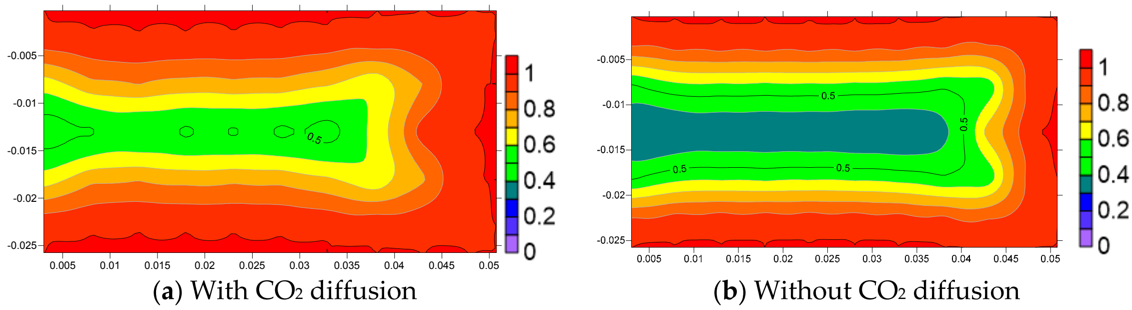

Figure 21. CO_2 global mole fraction of CO_2 huff-'n-puff in Case-4 in soaking process (ij profile).

- Capillary imbibition

According to Meng's research, in the presence of fractures the capillary force can play a role of imbibition, which can also promote the drainage process [39]. In comparison (Figure 22), oil recovery considering the imbibition effect is 1.3% higher than cases without considering it. From the water saturation profile (Figure 23) the matrix grids have higher water saturation with consideration of imbibition, which indicates that more water in the fracture may enter the matrix, and then impact the oil drainage.

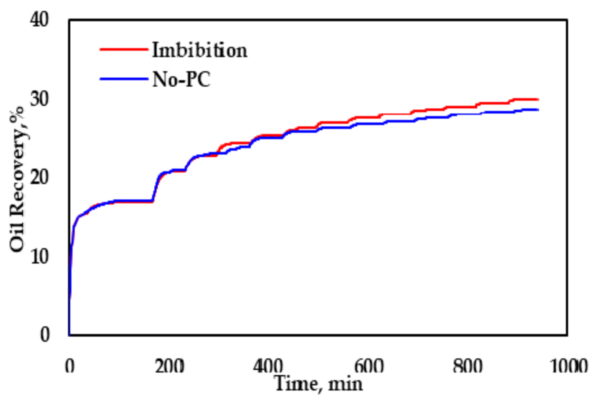

Figure 22. Oil recovery comparison of water huff-'n-puff with and without imbibition (Case-4).

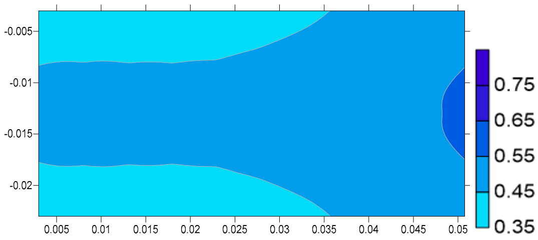

(**a**) With water imbibition (**b**) Without water imbibition

Figure 23. Water saturation of water huff-'n-puff in Case-4 in soaking process (ij profile).

- Gravity

Another observation of the water saturation profiles is that water can be imbibed and is subject to density differences in the water case, which can displace more oil towards the fracture. Water is denser than oil, and N_2 is less dense than oil. Aggregation of different phase during the soaking period may affect the performance of huff-'n-puff as well. By setting the $Kv = 1$, the permeability anisotropy is eliminated, and the difference between Case-4 and Case-7 is dominated by gravity effects. It can be seen from Figure 24 that the gravity effect is almost negligible in the depletion mode and the gas huff-'n-puff mode. In water huff-'n-puff, the oil recovery finally has a difference of 0.95% in Case-4 and Case-7. By comparing the oil saturation profiles of different layers (Figure 25), there are slight differences between top and bottom layers in CO_2 and N_2 huff-'n-puff, but the differences are not significant. The difference of saturation between top and bottom layers is more obvious in water huff-'n-puff. Thus, the gravity effect can be neglected in core scale model. Whether there is a significant impact on large size will be verified and discussed in the authors' later studies.

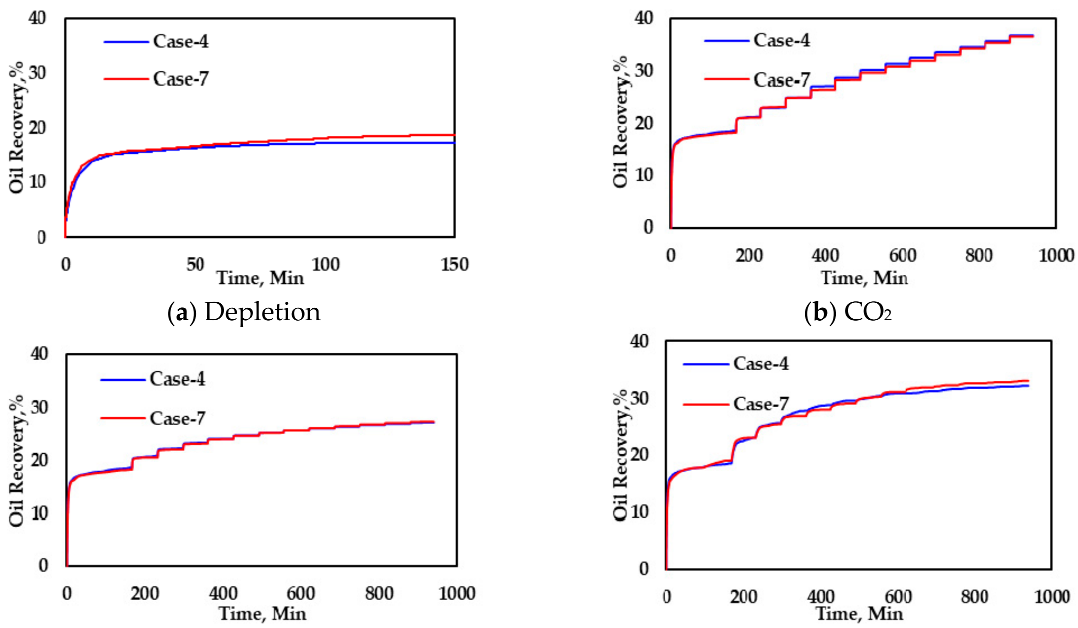

(**a**) Depletion (**b**) CO_2

(**c**) N_2 (**d**) Water

Figure 24. Oil recovery comparison with gravity effect.

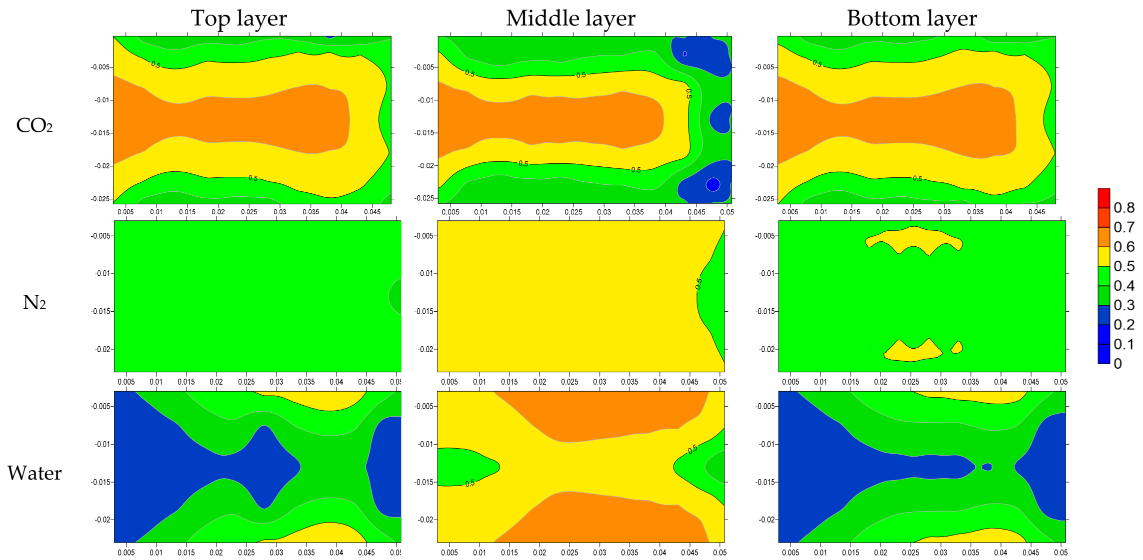

Figure 25. Oil saturation comparison with gravity effect (ij profile).

3.2. Fracture Characteristics

Now that the fundamental mechanisms of huff-'n-puff by using CO_2, N_2 and water are clear, it is of interest to understand how the distribution of fractures affects their performance in huff-'n-puff. For different fracture characteristics, the direction of scattered fracture, fracture in end face or lateral face, Scattered pattern of fractures, fracture relative location with well and fracture area are designed to mechanistically understand the impact of fracture characteristics on huff-'n-puff.

3.2.1. Scattered Pattern of Fractures

It is found that the dispersion characteristics of fractures has little effect on the recovery in N_2 and water huff-'n-puff. However, it has a great influence on the EOR effect in CO_2 case (Figure 26). When designing a fracture contact relationship, we compared four scattered fracture (Cases-1–4).

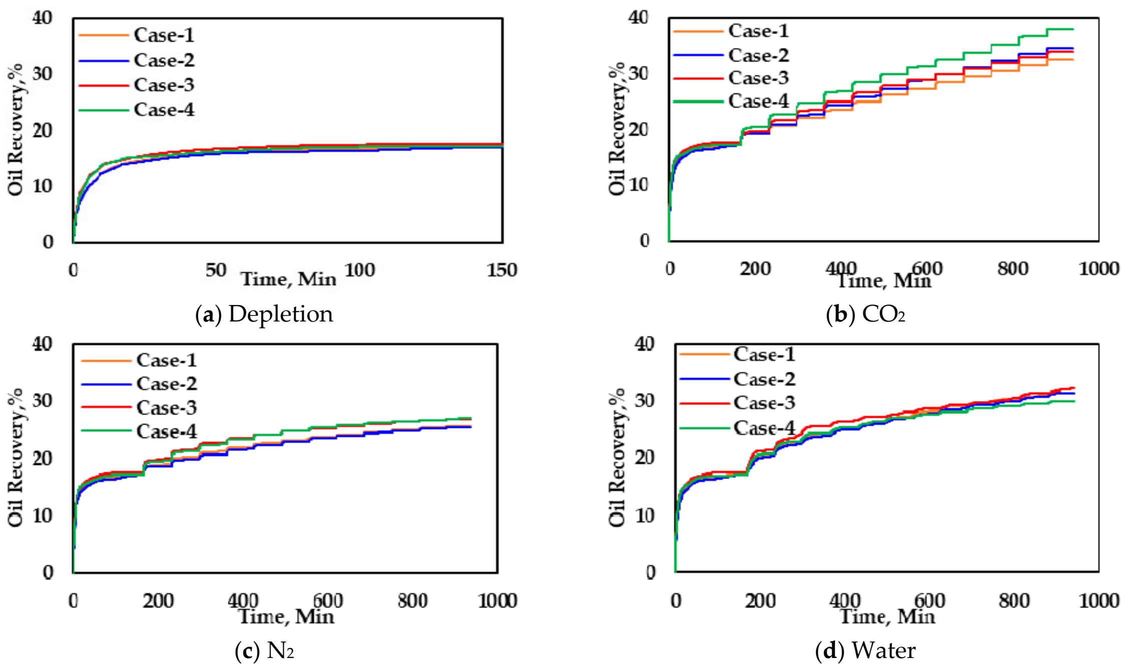

Figure 26. Oil recovery comparison between different scattered fractures.

In the depletion development mode, the final oil recoveries are not very different. In CO_2 huff-'n-puff, the oil recovery in Case-4 is the highest. The EOR effect in Case-1 is the worst. It can be seen from the comparison of CO_2 that the more scattered and farther in distance, the better the recovery effect of CO_2 huff-'n-puff. In N_2 huff-'n-puff cases, Case-3 and Case-4 are the best. In water huff-'n-puff cases, Case-4 is the best, followed by Case-3.

By comparing the oil viscosity distribution in different fractures (Figure 27), the fracture type in Case-4 can result in much less oil viscosity in the soaking process, and hence more oil can be produced. Therefore, the oil saturation is much lower in the Case-4 profile (Figure 28).

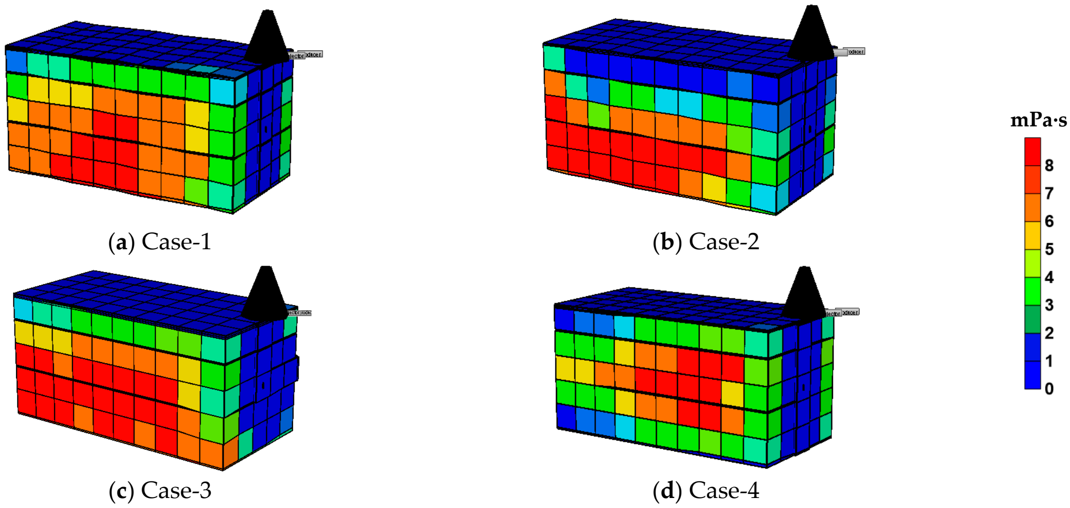

(**a**) Case-1 (**b**) Case-2

(**c**) Case-3 (**d**) Case-4

Figure 27. Oil viscosity comparison between different scattered fractures in the CO_2 soaking process.

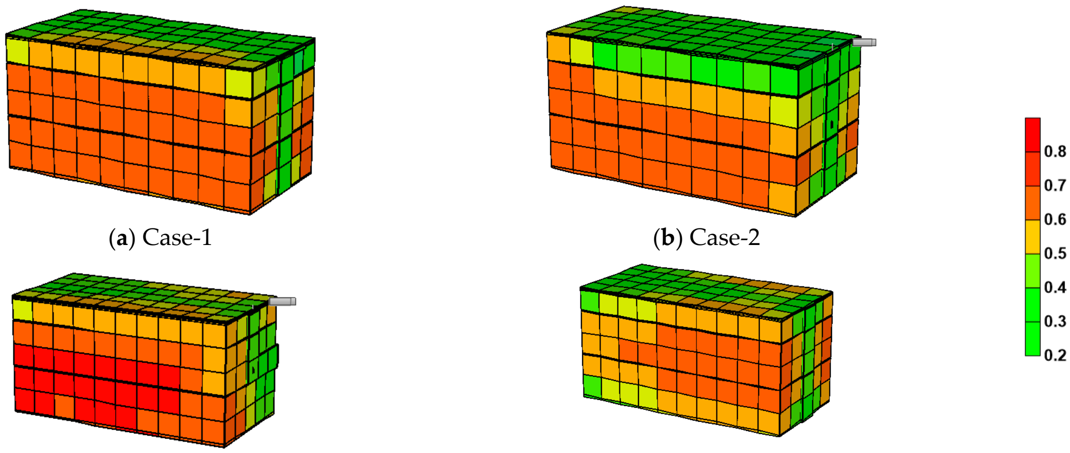

(**a**) Case-1 (**b**) Case-2

(**c**) Case-3 (**d**) Case-4

Figure 28. Oil Saturation comparison between different scattered fractures in CO_2 production process.

3.2.2. Direction of Scattered Fracture (with Kv = 0.2)

In this section, Case-4 and Case-7 are used to illustrate the mechanisms of permeability anisotropy by setting fractures in different directions. Figure 29 shows the oil recovery factor effect on surface conditions by using three different injecting fluids with fractures in different directions. The conclusion of this comparison is that permeability anisotropy plays a significant role in the water case (Case-7 is 4.38% higher than Case-4; but gravity has a negligible impact on CO_2 and N_2). The cross section of Cases-4 and -7 in *k*-*j* direction is specifically selected for analysis (Figures 30 and 31). From the viscosity comparison (Figure 30), the viscosity reduction area in Case-4 is larger than the area in Case-7.

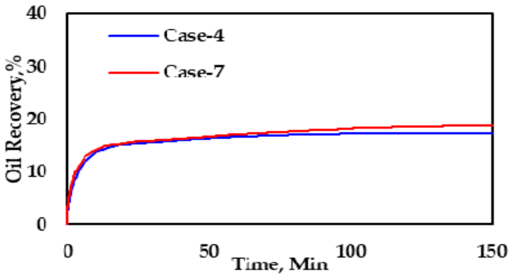

(**a**) Depletion

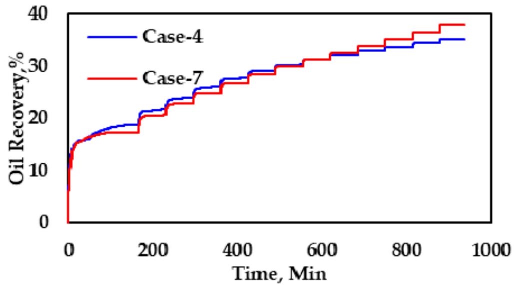

(**b**) CO_2

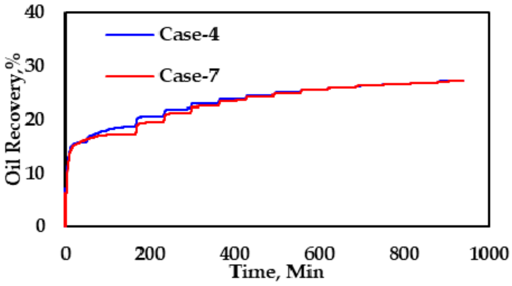

(**c**) N_2

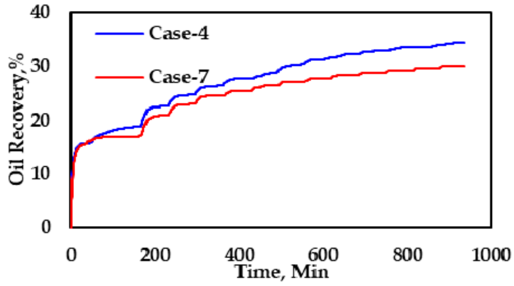

(**d**) Water

Figure 29. Oil recovery comparison between different directions of scattered fracture.

From the saturation profiles (Figure 31), it can be seen that in Case-4, more water can enter the matrix grid, but in Case-7 less oil can be displaced by water in this type fracture. As in the *Kv* and gravity effect, in Case-4, the oil recovery is significantly better than in Case-7. The fracture patterns in Cases-4 and -7 represent the typical horizontal well fracture and vertical well fracture. When it is extended to engineering applications, it can be considered that the horizontal well fractures are more effective than the vertical well fracture, and the horizontal fracture well is more suitable for water huff-n-puff. CO_2 huff-n-puff can be used both in horizontal and vertical fracture wells.

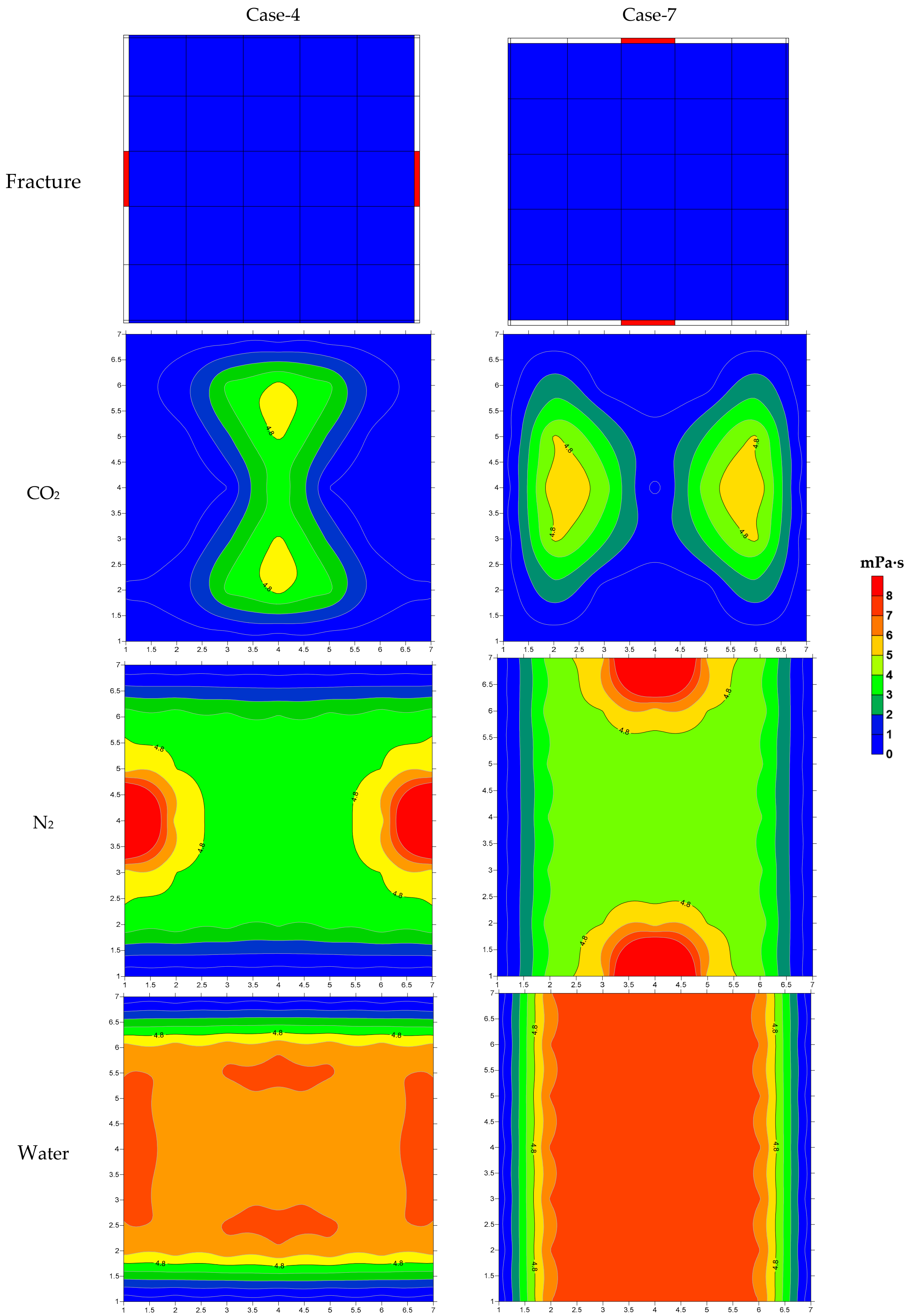

Figure 30. Oil viscosity of different fluids in soaking process (*jk* profile).

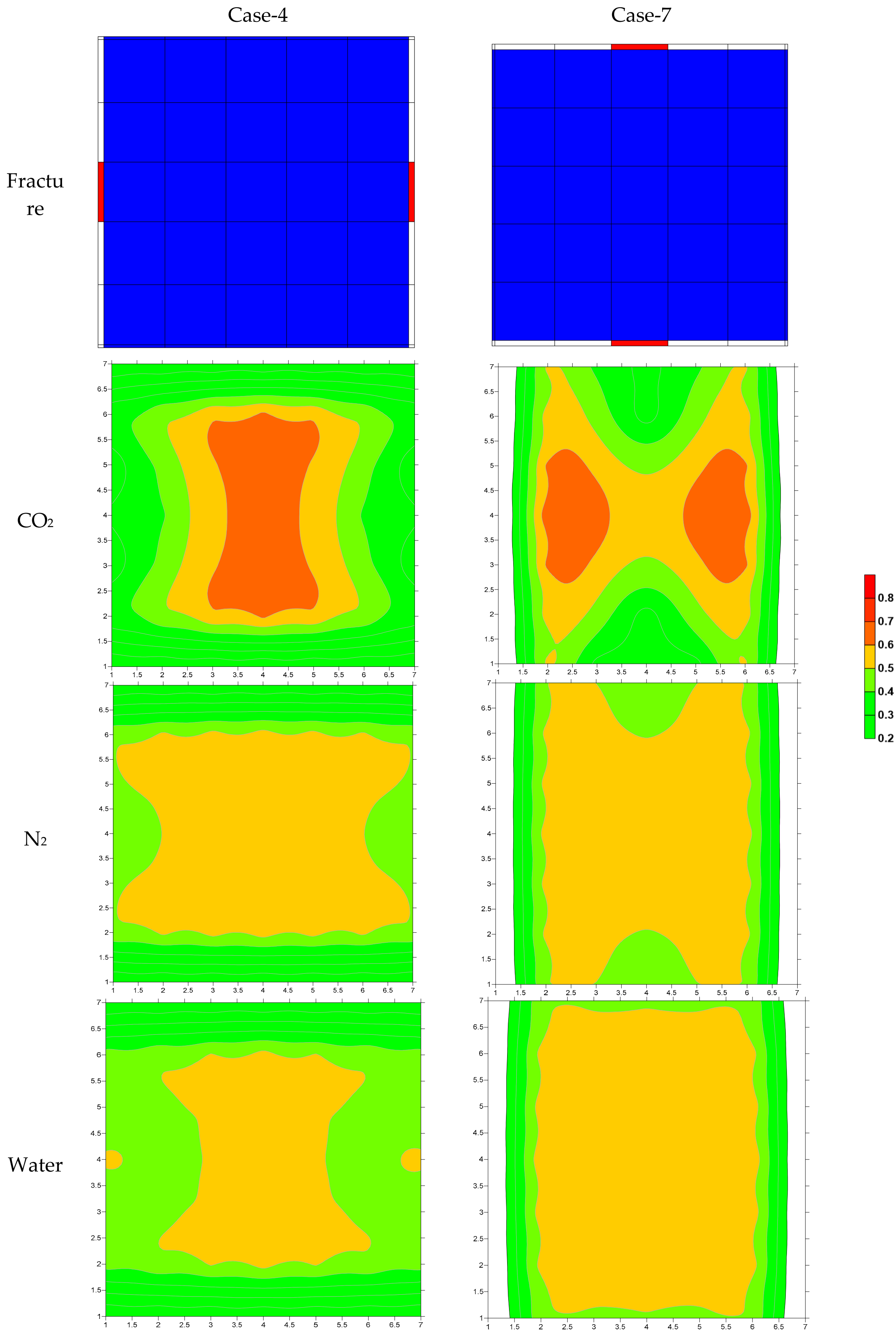

Figure 31. Oil saturation of different fluids in production process.

3.2.3. Fracture Near Well and Far Well

Due to the high conductivity of the fracture, the crude oil can flow into the well through the fractures, and the difference of oil recovery between the near-well and the far-well cases is small (Figure 32).

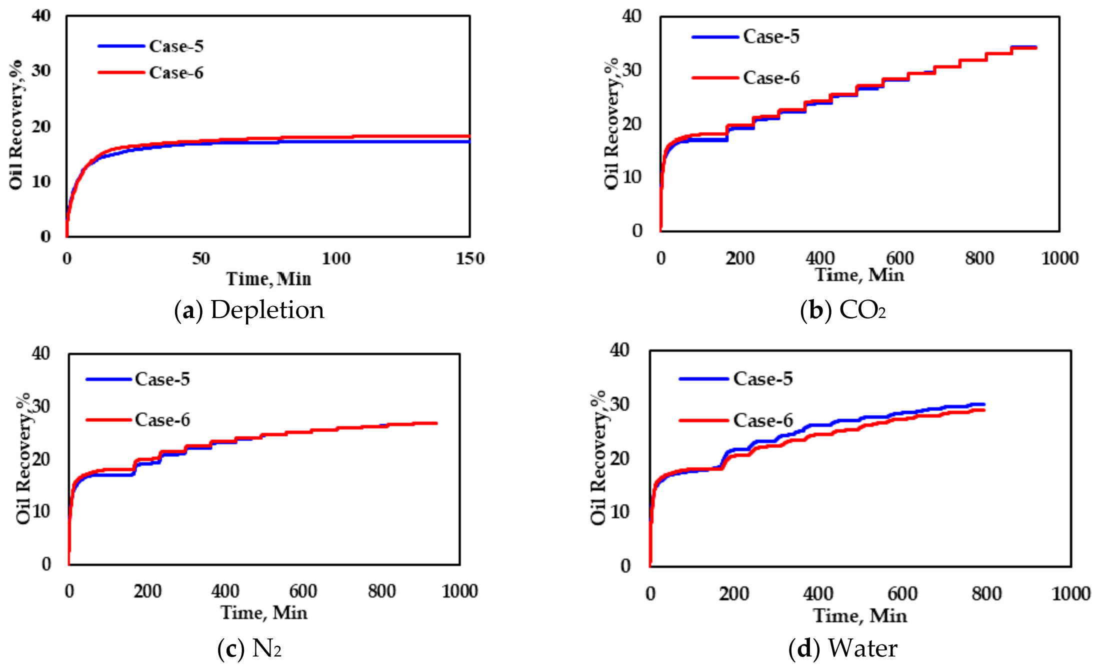

Figure 32. Oil recovery comparison between fractures near well and far well.

Comparing the EOR effects of near-well and far-well fracture in different development modes (Cases-5,6), it can be found that the results are not consistent either. For the depletion period, the far-well fracture (in Case-6) has an advantage over the near-well case (Case-5) by 1% higher oil recovery.

In the CO_2 and N_2 huff-''n-puff periods, the oil recovery of the two fracture types are close to each other. In water huff-'n-puff, the fracture in Case-5 has a higher incremental oil content. In the fourth round, the difference in oil recovery can even reach 3.1%, but in the later rounds, the difference is less than 0.74%.

3.2.4. Fracture Contact Area

Comparing the relationship between fracture contact area and oil recovery (Figure 33), it can be found that in the depletion period, the larger the contact area of the fracture, the higher the oil recovery, but when the contact area is greater than 25, the increase of the oil recovery is obviously slowed down. In the CO_2 huff-'n-puff, oil recovery is the highest when the contact area is 25. In N_2 and water huff-'n-puff, there is still not a clear trend between the contact area and oil recovery. Therefore, the contact area is not sensitive for the huff-'n-puff process based on this research.

3.2.5. Components Analysis

Through the previous comparison of oil recovery, viscosity, phase permeability and mobility, the EOR effect of different fluids in different fracture can be examined and compared macroscopically. In order to analyze the microscopic differences in more detail, we also selected Cases-4, 5 and 8 as the comparison experiments, adding the analysis of EOR produced components of different fluids in different fracture modes.

As can be seen from the figure (Figure 34), the mainly produced crude oil components include C7, C19 and C30. The proportion of C1 and C4 components in crude oil is originally small, and their production amount did not differ significantly between different fractures. First, for C7 analysis, the most component C7 can be produced in water huff-'n-puff, followed by CO_2, with the least amount of C7 produced during N_2 huff-'n-puff. For C19 and C30, CO_2 has a better drainage effect on them, followed by water, and N_2 is still the worst. This shows that different fluids have different drainage effects on different oil components. More interestingly, the fracture condition also has an effect on the composition of the components produced. Taking C19 as an example, C19 can be produced much easier in Case-5 in CO_2 huff-'n-puff. For water, the fracture in Case-8 is more conducive to the production of C19. This indicates that the fracture distribution pattern also has a non-negligible effect on the EOR effect of different fluids.

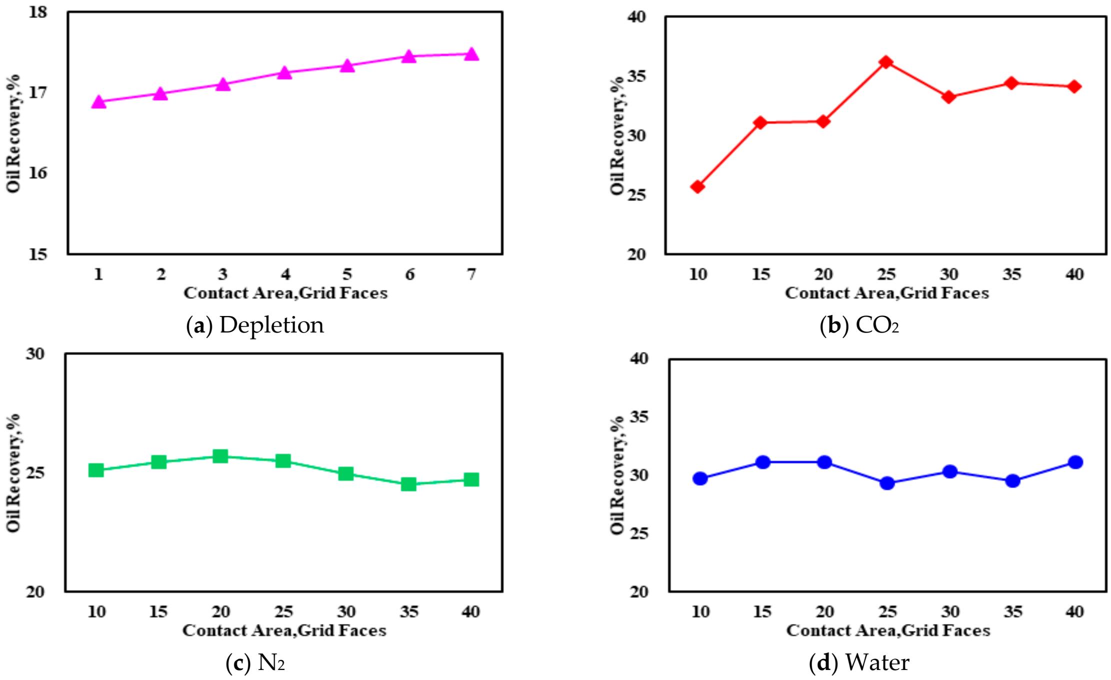

Figure 33. Relationship between contact area and oil recovery in different modes.

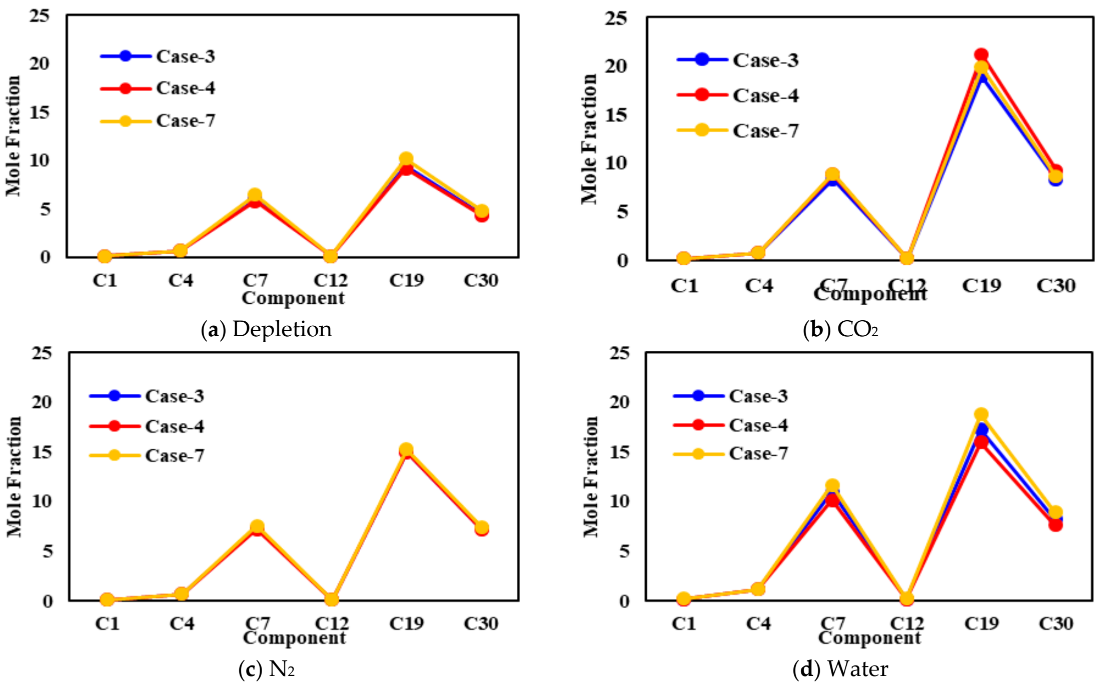

Figure 34. Production component comparison in different cases.

Finally, it should be noted that the main EOR effect is still due to the fluid. Fractures only provide a more efficient and convenient channel and contact relationship for fluids to exert their EOR effects. Finally, in the fluid selection of tight reservoir EOR huff-'n-puff, it is necessary to accurately and reasonably evaluate the distribution characteristics of fractures, and select the optimal injected fluid for specific fracture morphology.

4. Conclusions

This paper takes a fractured tight reservoir as the basic research object. Natural tight cores from the J field in China are used to conduct experimental studies on different fluid huff-'n-puff processes. A new experimental core-level fracture simulation method that is easy to operate and reusable is proposed. Three different injecting fluids are used, including CO_2, N_2 and water. The equivalent core scale reservoir numerical models in depletion and huff-'n-puff mode are then restored by numerical simulation with CMG GEM. Simulation cases with eight different fracture patterns were used in the detail study to understand how fracture mechanistically impact EOR in huff and puff for different injecting fluids including CO_2, N_2 and water. Finally, the key findings can be summarized as follows:

(1) In core-scale fractures, a new experimental core-level fracture simulation method that is easy to operate and reusable is proposed. In this method, woven metallic wires are attached to the outer surface of the core to create a space between the core holder and the core as a high permeability zone, equivalent to a fracture. This avoids the defects of single fracture shape, sanding, and difficulty in reusing the core. Different spatial arrangement of fractures can be set up in core-scale experiments.

(2) Based on the core-scale experiments and numerical simulation analyses, the existence of fractures is significant for the enhanced oil process in tight reservoirs. The presence of fractures not only has a significant effect on the depletion mode, but also has an important effect on the enhanced oil recovery (EOR) performance of the huff-'n-puff method. After comparison, fracture arrangement in space has most impact on CO_2 huff-'n-puff, followed by water and finally N_2.

(3) In the depletion mode, crude oil flows mainly due to the pressure drop caused by elastic energy, and there is no contact between other fluids and crude oil in the matrix through fractures. Therefore, in the case of depletion mode, when fractures have the same contact area with spatial arrangement, the obvious difference in oil recovery cannot be observed.

(4) CO_2 has more advantages over water and N_2 in tight reservoir with huff-'n-puff. Through the EOR mechanism analysis, CO_2 is the only fluid that is miscible with oil (even a 90% mole fraction with CO_2 in the oil phase is possible). This solubility of CO_2 results in the lowest oil phase viscosity in the three cases. The CO_2 diffusion mechanism is pronounced. In contrast, N_2 mainly exists in the gas phase and is much less soluble in the oil phase compared to CO_2, however, it still has a certain swelling effect on crude oil. Water does not dissolve in the oil and water mainly enhances oil recovery through capillary force, gravity and elasticity displacement.

(5) When considering the anisotropy, the direction of fracture will have a greater impact on oil recovery for the water huff-'n-puff. The conclusion from this comparison is that permeability anisotropy plays a significant role in the water case (Case-7 is 4.38% higher than Case-4; but anisotropy has a negligible impact on CO_2 and N_2).

(6) When it comes to the relative location between well and fracture, for the depletion development mode, the far-well fracture has an advantage over the near well case by 1% higher oil recovery. In the CO_2 and N_2 huff-'n-puff modes, the oil recovery of the two fracture types are not much different. In water huff-'n-puff, the fractures near the well have a better effect on the EOR process.

(7) The fracture contact area is not sensitive for the huff-'n-puff process for N_2 and water cases based on this research.

(8) From analysis of the produced components, CO_2 gives the most incremental C19 and C30 compared to depletion. However, in the water case, more C7 are produced, leaving a depleted

heavy mass that causes an increase in the viscosity of the crude oil. N_2 has the least incremental effect oil components for all carbon number ranges.

(9) Finally, the main EOR effect is mainly applied by the fluid. Fractures only provide a more efficient and convenient channel, and offer a better contact relationship for fluids to exert their EOR effects. In the fluid selection of tight reservoir EOR huff-n-puff, it is necessary to accurately and reasonably evaluate the distribution characteristics of fractures, and select the optimal injected fluid for specific fracture morphology.

Author Contributions: Conceptualization, J.B. and H.L.; Methodology, J.B.; Software, J.B.; Validation, L.Y. and F.C.; Formal Analysis, H.L.; Investigation, J.B.; Resources, G.Q. and Y.P.; Data Curation, Y.G.; Writing—Original Draft Preparation, J.B.; Writing—Review & Editing, H.L.; Visualization, J.B.; Supervision, J.W.; Project Administration, G.Q.; Funding Acquisition, G.Q.

Funding: This research was funded by National Program on Key Basic Research Project (No. 2015CB250906) and Innovation Fund of CNPC (No. 2015D-5006-0204).

Acknowledgments: We thank the teams at PetroChina Xinjiang Oilfield and Beijing RIPED.

Conflicts of Interest: The authors declare no conflict of interest.

References

1. Pollastro, R.M. Total petroleum system assessment of undiscovered resources in the giant Barnett Shale continuous (unconventional) gas accumulation, Fort Worth Basin, Texas. *AAPG Bull.* **2007**, *91*, 551–578. [CrossRef]
2. Miller, B.; Paneitz, J.; Mullen, M.; Meijs, R.; Tunstall, K.; Garcia, M. The Successful Application of a Compartmental Completion Technique Used to Isolate Multiple Hydraulic-Fracture Treatments in Horizontal Bakken Shale Wells in North Dakota. In Proceedings of the SPE Annual Technical Conference and Exhibition, Denver, CO, USA, 21–24 September 2008.
3. Loucks, R.G.; Reed, R.M.; Ruppel, S.C.; Jarvie, D.M. Morphology, Genesis, and Distribution of Nanometer-Scale Pores in Siliceous Mudstones of the Mississippian Barnett Shale. *J. Sediment. Res.* **2009**, *79*, 848–861. [CrossRef]
4. Jia, C.; Caineng, Z.; Jianzhong, L.; Denghua, L.; Min, Z. Evaluation criteria, main types, basic characteristics and resource prospects of China's tight oil. *Acta Pet. Sin.* **2012**, *33*, 343–350.
5. Hawthorne, S.B.; Gorecki, C.D.; Sorensen, J.A.; Miller, D.J.; Harju, J.A.; Melzer, L.S. Hydrocarbon Mobilization Mechanisms from Upper, Middle, and Lower Bakken Reservoir Rocks Exposed to CO. In Proceedings of the SPE Unconventional Resources Conference Canada, Calgary, AB, Canada, 5–7 November 2013.
6. Jinhu, D.; Haiqing, H.; Jianzhong, L.; Fuji, H.; Bingcheng, G.; Weipeng, Y. Progress in China's Tight Oil Exploration and Challenges. *China Pet. Explor.* **2014**, *19*, 1–9.
7. Rungamornrat, J.; Wheeler, M.F.; Mear, M.E. Coupling of Fracture/Non-Newtonian Flow for Simulating Nonplanar Evolution of Hydraulic Fractures. In Proceedings of the SPE Annual Technical Conference and Exhibition, Dallas, TX, USA, 9–12 October 2005.
8. Kabir, S.; Rasdi, F.; Igboalisi, B.O. Analyzing Production Data from Tight Oil Wells. *J. Can. Pet. Technol.* **2011**, *50*, 48–58. [CrossRef]
9. West, D.R.; Harkrider, J.D.; Barham, M.; Besler, M.R.; Mahrer, K.D. Optimized Production in the Bakken Shale: South Antelope Case Study. In Proceedings of the SPE Unconventional Resources Conference Canada, Calgary, AB, Canada, 5–7 November 2013.
10. Wang, H.; Liao, X.; Lu, N.; Cai, Z.; Liao, C.; Dou, X. A study on development effect of horizontal well with SRV in unconventional tight oil reservoir. *J. Energy Inst.* **2014**, *87*, 114–120. [CrossRef]
11. Wei, Y.; Ran, Q.; Ran, L.I.; Yuan, J.; Dong, J. Determination of dynamic reserves of fractured horizontal wells in tight oil reservoirs by multi-region material balance method. *Pet. Explor. Dev.* **2016**, *43*, 490–498. [CrossRef]
12. Sohrabi, M.; Tehrani, D.H.; Danesh, A.; Henderson, G.D. Visualisation of Oil Recovery by Water Alternating Gas (WAG) Injection Using High Pressure Micromodels—Oil-Wet & Mixed-Wet Systems. In Proceedings of the SPE Annual Technical Conference and Exhibition, New Orleans, LA, USA, 30 September–3 October 2001.

13. Ghaderi, S.M.; Clarkson, C.R.; Kaviani, D. Evaluation of Recovery Performance of Miscible Displacement and WAG Processes in Tight Oil Formations. In Proceedings of the SPE/EAGE European Unconventional Resources Conference and Exhibition, Society of Petroleum Engineers, Vienna, Austria, 20–22 March 2012.
14. Holtz, M.H. Immiscible Water Alternating Gas (IWAG) EOR: Current State of the Art. In Proceedings of the SPE Improved Oil Recovery Conference, Tulsa, OK, USA, 11–13 April 2016.
15. Yu, W.; Lashgari, H.R.; Wu, K.; Sepehrnoori, K. CO_2 injection for enhanced oil recovery in Bakken tight oil reservoirs. *Fuel* **2015**, *159*, 354–363. [CrossRef]
16. Hoffman, B.T. Comparison of Various Gases for Enhanced Recovery from Shale Oil Reservoirs. In Proceedings of the SPE Improved Oil Recovery Symposium, Society of Petroleum Engineers, Tulsa, OK, USA, 14–18 April 2012.
17. Arshad, A.; Al-Majed, A.A.; Menouar, H.; Muhammadain, A.M.; Mtawaa, B. Carbon Dioxide (CO_2) Miscible Flooding in Tight Oil Reservoirs: A Case Study. In Proceedings of the Kuwait International Petroleum Conference and Exhibition, Kuwait City, Kuwait, 14–16 December 2009.
18. Song, C.; Yang, D. Performance Evaluation of CO_2 Huff-n-Puff Processes in Tight Oil Formations. In Proceedings of the SPE Unconventional Resources Conference Canada, Calgary, AB, Canada, 5–7 November 2013.
19. Wang, H.; Liao, X.; Lu, N.; Cai, Z.; Liao, C.; Dou, X. The Study of CO_2 Flooding of Horizontal Well with SRV in Tight Oil Reservoir. In Proceedings of the SPE Energy Resources Conference, Port of Spain, Trinidad and Tobago, 9–11 June 2014.
20. Ren, B.; Ren, S.; Zhang, L.; Huang, H.; Chen, G.; Zhang, H. Monitoring on CO_2 Migration in a Tight Oil Reservoir during CO_2-EOR Process. In Proceedings of the Carbon Management Technology Conference, Carbon Management Technology Conference: Sugar Land, TX, USA, 17–19 November 2015.
21. Sheng, J.J. Enhanced oil recovery in shale reservoirs by gas injection. *J. Nat. Gas Sci. Eng.* **2015**, *22*, 252–259. [CrossRef]
22. Yang, Z.; Liu, X.; Zhang, Z.H.; Zhou, T.; Zhao, S.X. Physical simulation of CO_2 injection in fractureing horizontal wells in tight oil reservoirss. *Acta Pet. Sin.* **2015**, *36*, 724–729.
23. Torabi, F.; Asghari, K. Performance of CO_2 Huff-and-Puff Process in Fractured Media (Experimental Results). In Proceedings of the Canadian International Petroleum Conference, Petroleum Society of Canada: Calgary, AB, USA, 12–14 June 2007; p. 11.
24. Gamadi, T.D.; Sheng, J.J.; Soliman, M.Y. An Experimental Study of Cyclic CO_2 Injection to Improve Shale Oil Recovery. In Proceedings of the SPE Improved Oil Recovery Symposium, Society of Petroleum Engineers: Tulsa, OK, USA, 12–16 April 2014; p. 9.
25. Ma, J.; Wang, X.Z.; Gao, R.M.; Zeng, F.H.; Huang, C.X.; Tontiwachwuthikul, P.; Liang, Z.W. Enhanced light oil recovery from tight formations through CO_2 huff 'n' puff processes. *Fuel* **2015**, *154*, 35–44. [CrossRef]
26. Todd, H.B.; Evans, J.G. Improved Oil Recovery IOR Pilot Projects in the Bakken Formation. In Proceedings of the SPE Low Perm Symposium, Society of Petroleum Engineers: Denver, CO, USA, 5–6 May 2016; p. 22.
27. Wang, L.; Tian, Y.; Yu, X.Y.; Wang, C.; Yao, B.W.; Wang, S.H.; Winterfeld, P.H.; Wang, X.; Yang, Z.Z.; Wang, Y.H. Advances in improved/enhanced oil recovery technologies for tight and shale reservoirs. *Fuel* **2017**, *210*, 425–445. [CrossRef]
28. Hawthorne, S.B.; Gorecki, C.D.; Sorensen, J.A.; Steadman, E.N.; Harju, J.A.; Melzer, S. Hydrocarbon Mobilization Mechanisms Using CO_2 in an Unconventional Oil Play. *Energy Procedia* **2014**, *63*, 7717–7723. [CrossRef]
29. Yu, W.; Lashgari, H.; Sepehrnoori, K. Simulation Study of CO_2 Huff-n-Puff Process in Bakken Tight Oil Reservoirs. In Proceedings of the SPE Western North American and Rocky Mountain Joint Meeting, Denver, CO, USA, 17–18 April 2014.
30. Tovar, F.D.; Eide, O.; Graue, A.; Schechter, D. Experimental Investigation of Enhanced Recovery in Unconventional Liquid Reservoirs using CO_2: A Look Ahead to the Future of Unconventional EOR. In Proceedings of the SPE Unconventional Resources Conference, Society of Petroleum Engineers: The Woodlands, TX, USA, 1–3 April 2014; p. 9.
31. Vega, B.; O'Brien, W.J.; Kovscek, A.R. Experimental Investigation of Oil Recovery from Siliceous Shale by Miscible CO_2 Injection. In Proceedings of the SPE Annual Technical Conference and Exhibition, Society of Petroleum Engineers: Florence, Italy, 19–22 September 2010; p. 21.

32. Gamadi, T.D.; Sheng, J.J.; Soliman, M.Y. An Experimental Study of Cyclic Gas Injection to Improve Shale Oil Recovery. In Proceedings of the SPE Annual Technical Conference and Exhibition, New Orleans, LA, USA, 30 September–2 October 2013; p. 9.
33. Lei, L.; Sheng, J.J. Upscale Methodology for Gas Huff-n-Puff Process in Shale Oil Reservoirs. *J. Pet. Sci. Eng.* **2017**, *153*, 36–46. [CrossRef]
34. Jing, W. Investigations on spontaneous imbibition and the influencing factors in tight oil reservoirs. *Fuel* **2019**, *236*, 755–768. [CrossRef]
35. Jing, W.; Huiqing, L.; Genbao, Q.; Yongcan, P.; Yang, G. Experimental investigation on water flooding and continued EOR techniques in buried-hill metamorphic fractured reservoirs. *J. Pet. Sci. Eng.* **2018**, *171*, 529–541.
36. Kurtoglu, B.; Salman, A. How to Utilize Hydraulic Fracture Interference to Improve Unconventional Development. In Proceedings of the Abu Dhabi International Petroleum Exhibition and Conference, Society of Petroleum Engineers: Abu Dhabi, The United Arab Emirates, 9–12 November 2015; p. 18.
37. Wei, B.; Li, Q.; Jin, F.; Li, H.; Wang, C. The Potential of a Novel Nanofluid in Enhancing Oil Recovery. *Energy Fuels* **2016**, *30*, 2882–2891. [CrossRef]
38. Meng, Q.; Cai, Z.X.; Cai, J.C.; Yang, F. Oil recovery by spontaneous imbibition from partially water-covered matrix blocks with different boundary conditions. *J. Pet. Sci. Eng.* **2019**, *172*, 454–464. [CrossRef]
39. Weng, X.W.; Kresse, O.; Cohen, C.E.; Wu, R.T.; Gu, H.R. Modeling of Hydraulic-Fracture-Network Propagation in a Naturally Fractured Formation. *SPE Prod. Oper.* **2011**, *26*, 368–380.
40. Zuloaga-Molero, P.; Yu, W.; Xu, Y.; Sepehrnoori, K.; Li, B. Simulation Study of CO_2-EOR in Tight Oil Reservoirs with Complex Fracture Geometries. *Sci. Rep.* **2016**, *6*, 33445. [CrossRef] [PubMed]
41. CMG. *CMG: User's Guide GEM*; Computer Modeling Group, Ltd.: Calgary, AB, Canada, 2015.
42. Sigmund, P.M. Prediction of Molecular Diffusion at Reservoir Conditions. Part II—Estimating the Effects of Molecular Diffusion and Convective Mixing in Multicomponent Systems. *J. Can. Pet. Technol.* **1976**, *15*, 11. [CrossRef]
43. Reid, R.C.; Sherwood, T.K. The properties of gases and liquids: Their estimation and correlation. *Phys. Today* **1959**, *12*, 38–40. [CrossRef]
44. Zhang, Y.; Yu, W.; Li, Z.P.; Sepehrnoori, K. Simulation study of factors affecting CO_2 Huff-n-Puff process in tight oil reservoirs. *J. Pet. Sci. Eng.* **2018**, *163*, 264–269. [CrossRef]
45. Li, S.; Li, Z.; Dong, Q. Diffusion coefficients of supercritical CO_2 in oil-saturated cores under low permeability reservoir conditions. *J. CO_2 Util.* **2016**, *14*, 47–60. [CrossRef]